

Building an Understanding of Human-Water Resource Relationships  
through Community Engagement in Ha‘ikū and Huelo, HI

A THESIS SUBMITTED TO THE GRADUATE DIVISION OF THE  
UNIVERSITY OF HAWAI‘I AT MĀNOA IN PARTIAL  
FULFILLMENT  
OF THE REQUIREMENTS FOR THE DEGREE OF  
MASTER OF SCIENCE  
IN  
EARTH AND PLANETARY SCIENCE  
December 2024

By  
Brandon Bees

Thesis Chair:  
Christopher Shuler  
Thesis Committee:  
Henrietta Dulai  
Xiaolong Geng  
Diamond Tachera

## Preface: Community and Research Scope

This thesis represents not just an academic endeavor but a community-driven project that is deeply engaged with the residents of Ha‘ikū and Huelo. The project's primary goal was to co-produce usable, place-based water resources data with the Ha‘ikū Community Association (HCA) by leveraging local networks and incorporating the knowledge of residents in the research design. The insights and historical knowledge provided by the HCA board and individual community members were instrumental in shaping the study and its outcomes. The engagement process included meetings and feedback sessions, ensuring that the community's voice was heard and integrated into the project's methodology and interpretation of results. For example, the community was the primary source of knowledge for identifying sample locations. By involving the community in data collection and discussion of results, this project hopes to foster a sense of ownership and collaboration.

This thesis marks the beginning of what we hope will be a larger, ongoing project with a goal at enhancing community involvement in water resource management. **The findings and data produced here are a start towards developing a community-driven understanding of water in the Ha‘ikū and Huelo region, and represent only the beginning in terms of truly understanding this diverse and hydrologically complicated region. While not comprehensive, this work serves as a foundation for future research and community initiatives, ensuring that the residents of Ha‘ikū and Huelo continue to benefit from and contribute to the understanding and preservation of their water resources.**

This ongoing commitment to community collaboration highlights the project's broader impact and ensures that the knowledge generated remains accessible and beneficial to those who need it most. The continuation of this project beyond the scope of this thesis will aim to address emerging challenges and leverage new opportunities for sustainable water management in Northeast Maui.

# Abstract

This community-funded project is in support of the Ha‘ikū and Huelo residents that are impacted by limitations in, and decreasing quality of their drinking water sources. In the study area, many homes are not served by the County water system, and thus rely on private wells, springs, or rain catchment. The potential for future water development in northeast Maui, Hawai‘i, causes concern for residents reliant on private ground or surface water sources. The vulnerability of water resources to overexploitation may cause negative impacts on both the water availability and cultural practices in this region. By supporting local residents in developing a better understanding of aquifer characteristics and response to stresses, such as decreased rainfall, or increased withdrawal rate, this work aims to increase community capacity and boost future water resilience. Increased knowledge of the hydrological connections that exist throughout the aquifer will yield insights into how future water withdrawals may impact current water levels and uses. Here, we use analysis of water isotopes ( $^2\text{H}$  and  $^{18}\text{O}$ ) in groundwater, surface water and precipitation, as well as major ion composition to elucidate connectivity between surface water and groundwater in the study region. We also applied an existing MODFLOW model to examine the impacts of a set of hypothetical production wells at different pumping rates to simulate how current wells may be affected under hypothetical scenarios of future water development. We conducted an analysis of historical rainfall data and future projections to consolidate data and discuss trends and the effects of ENSO on precipitation. Overall, results suggest that groundwater and surface water in Ha‘ikū are unlikely to be hydrologically connected due to statistically different geochemistry, which suggests that they originate from different source areas and elevations. However, in Huelo the opposite is found suggesting there may be different hydrogeologic or climatic factors that control groundwater-surface water interactions in different places. Groundwater model results indicate that the impact of future withdrawals can vary dramatically based on the geographic location of pumping wells and residential wells. These challenges all fall under the backdrop of decreasing rainfall trends between 1920 and present.

# Table of Contents

Preface: Community and Research Scope	2
<b>Abstract</b>	<b>3</b>
<b>Table of Contents</b>	<b>6</b>
<b>Introduction</b>	<b>7</b>
I. Study Motivation	7
II. Community Concerns	8
III. Community Involvement	9
IV. Isotopic Analysis of Aquifer Systems	10
V. Groundwater Modeling	10
VI. Impact of Climate Change on Groundwater Resources	11
VII. Hypotheses and Objectives	14
<b>Methods</b>	<b>15</b>
I. Sample Collection and Lab Analysis	15
II. Historical Precipitation Record	19
III. Groundwater Modeling Methods	21
<b>Results</b>	<b>25</b>
I. Potential Hydraulic Connections	25
A. Precipitation	25
Precipitation Isotopes Volumetric, 18O Content and Temporal Variability	25
B. Precipitation Isotope Content	26
Terrestrial Samples	30
C. Monthly Repeated Samples	34
D. Similarities and Differences of Major Ions	36
E. Results of Analysis of Stable Isotopes and Major Ions	37
Stream and Well Water Level Comparison	39
Limitations	41

II. Groundwater Model and Future Scenarios	41
A. Groundwater Scenario Results	41
Limitations	43
III. Precipitation Analysis	43
A. Historical Precipitation and Trends in Subregions	43
B. Local Precipitation Variation with ENSO	48
Future Precipitation Projections	51
Limitations	53
<b>Discussion</b>	<b>53</b>
I. Areas of Interest	54
Isotope Results in Reference to Previous Studies	57
II. Hydrologic Framework and Groundwater Movement	58
III. Precipitation Changes with Reference to ENSO Phase Changes	59
IV. Simulated Impacts on Existing Wells	59
<b>Conclusions</b>	<b>60</b>
<b>Acknowledgements</b>	<b>61</b>
<b>References</b>	<b>62</b>
<b>Appendix</b>	<b>68</b>

# Introduction

## I. Study Motivation

Access to clean and abundant water is fundamental for sustaining human populations, and changes in water quality and quantity have direct and far-reaching impacts. The world is witnessing an increasing scarcity of freshwater resources due to the combined effects of a growing population and a changing climate (Boretti & Rosa, 2019). Already, access to freshwater is being cut off to many people around the world (Gleick & Palaniappan, 2010). Freshwater is a resource vulnerable to natural and anthropogenic impacts. Urbanization and other anthropogenic effects are changing the balance between groundwater recharge and runoff (Chen et al., 2017). The global challenge of water access is exacerbated by both natural and human-induced factors. The U.S. State of Hawaii has limited access to freshwater due to its situation as an archipelago in the Pacific Ocean, far from any continents (Izuka et al., 2018).

Ha‘ikū-Pauwela, referenced here as just Ha‘ikū, is a small community on the north shore of the Hawaiian island of Maui. Access to freshwater is becoming a critical community issue because urbanization, development pressure, and anthropogenic climate change are exacerbating historical inequalities in water distribution and control throughout the island of Maui. This has led to a renewed and revived interest amongst the Ha‘ikū and Huelo communities to better understand how these factors may impact their access to water and quality of living into the future.

## II. Community Concerns

The Maui County Department of Water Supply acknowledges the need for more water to accommodate population and agriculture growth in the Maui Island Water Use & Development Plan, as outlined in the Executive Summary of Ordinance 5335 (Maui County Board of Water Supply, 2021). As a result of this need, the Maui County Department of Water Supply has identified drilling new municipal scale wells in the Ha‘ikū area as a potential water source strategy within the Maui Water Plan. (Hui Alanui o Makena et al., 2003). However,

this proposition raises concerns among potentially affected communities, especially those residents reliant on private water sources like wells, springs, and catchment systems. Residents note that the 2019 Draft of Ordinance 5335 acknowledges a lack of hydrogeological and future climate information on the potential impacts of water development on private water sources, thereby increasing community concerns about any proposed plans (Maui County Board of Water Supply, 2019). There is precedence for community skepticism about development of water resources. According to a letter that was received by Maui Senator, Lynn DeCoite, the diversion of water from streams to plantation land for decades has already cut off families from vital water sources (Townsend, 2016). The Ha'ikū and Huelo communities have historically faced multifaceted challenges to local-scale water sovereignty including region-to region water transfers, loss of water for traditional Hawaiian kalo (taro) farming, and lack of water security in the context of a changing climate. The lineal descendants, current residents, and domestic waters users of northeast Maui have been for many years, and still are concerned about their livelihoods that all depend on access to freshwater.

While diversion of streams is not the focus of this report, the history of water in the region, and local sentiment regarding water are closely tied to issues surrounding inter-basin transfers of surface waters. Agricultural water diversions from streams, resulting in their drying out, impacts Hawaiian cultural practices. Freshwater streams have been used for traditional uses in Hawai'i throughout the recorded history of human settlement in these islands (Jones et al., 2015). Kalo farming in lo'i, otherwise known as irrigated terrace farming, is one of the most important water uses to the Hawaiian people that produces a staple crop of cultural significance. Some kalo farmers in Maui are currently experiencing water issues. One Wailuku farmer's stream stopped flowing and they discovered a lock and chain on a diversion upstream, preventing water from reaching the kalo (Davis, 2021). Loss of water in some streams causes serious consequences for kalo farmers, including loss of income, loss of a staple food, and lost opportunities for cultural practices.

Over 90% of streams have been diverted in Maui to deliver water to agricultural areas (Maui County Department of Water Supply, 2019). In addition, a decreasing trend of base

flow was found in streams across the Hawaiian Islands from 1913-2008 that is thought to be a sign of lower total rainfall and lower groundwater availability (Bassiouni & Oki, 2013). The flow of water in the streams of northeast Maui in many ways, dictates the quality of life for residents.

### III. Community Involvement

In order to fund this research, the Haiku Community Association (HCA) raised funds within their community to address important water resource concerns and to create scientific knowledge that could be used to support decisions and educate residents. For this study, our research team met with board members of HCA to define the study scope and identify key topics such as well and stream hydrogeologic connections, changes in historical rainfall, and vulnerability of private wells to future municipal-scale pumping.

In response to the questions that were posed, we co-developed methods to collect data and involve local residents. Not all topics that the community was interested in could be addressed within this study because of budgetary constraints or limitations in capacity. For example, potential water contamination by Dibromochloropropane (DBCP), a historical pineapple field nematicide used in the area, is an important concern, but could not be addressed in this study due to limitations in time and funds. Thus, the work we were able to conduct within the scope of this study represents a start towards developing a more complete understanding of the complex and poorly constrained hydrogeology and climatology of Northeastern Maui. Our study is the beginning to what we hope is a long and fruitful continued community-led exploration of the waters used by and cared for by the people of Ha'ikū and Huelo.

### IV. Isotopic Analysis of Aquifer Systems

As new wells are drilled and more water is withdrawn from the aquifer the water table decreases, potentially drying streams or preventing existing wells from reaching water. Understanding aquifer characteristics is crucial for managing water resources effectively.

Insights can be gained through comparison of the water quality parameters between water samples collected from different sources and in different places. Stable isotopes of hydrogen and oxygen offer valuable insights into the fractionation history of different water sources and the elevation at which the processes of condensation, precipitation, and recharge may have taken place. (Yeh & Lee, 2018). Previous studies in Maui and Hawai'i Island have explored the geochemical variability of perched water bodies and basal water, shedding light on expected stable water isotope variation due to elevation and location of precipitation on these islands that are dramatically affected by steep rainfall gradients driven by orographic rainfall patterns (Scholl et al., 1996; Scholl et al., 2002; Niu et al., 2017).

## V. Groundwater Modeling

The close proximity of multiple wells draws down the local water table, causing a cone of depression below the well surrounding wells (Baalousha, 2012). Groundwater models are commonly used to assess how groundwater resources can be affected by changes in water availability due to anthropogenic forcing. Predicting how wells will respond to changes in recharge and the impacts of nearby well pumping is visualized using software such as MODFLOW. Ke et al. performed a theoretical study that used a saturated-unsaturated coupling model for groundwater flowing into seepage wells to understand groundwater development in river basins and found that large groundwater withdrawals may cause the river to become disconnected from the groundwater, creating an unsaturated zone, thus decreasing the efficiency of the seepage wells (2021). Gingerich created multiple withdrawal scenarios at varying pumping rates and locations for the freshwater lens in Wailuku, Hawaii, and found that continuing 1996 and 2000 groundwater withdrawals would decrease water levels and produce a thinner freshwater lens (2008). A numerical groundwater model that simulated the freshwater lens was constructed by Rotzoll et al. constructed a numerical groundwater model to better understand the changes in flow and salinity in central Maui in response to planned withdrawal increases and found that higher future simulated withdrawals led to less available groundwater and higher groundwater salinity concentrations.

## VI. Impact of Climate Change on Groundwater Resources

More than 90% of the state of Hawaii has experienced a decrease in precipitation between 1920-2012 (Frazier & Giambelluca 2017). Climate change introduces additional stressors on groundwater resources, including sea level rise and regional climate shifts. Regional climate phenomena, like drought, stress local water supplies. The average air temperature in the Hawaiian Islands has increased between 1996-2006, rainfall has decreased since the 20th century, dry periods have become longer, base flow has decreased, and groundwater recharge and storage has decreased (Keener et al., 2012). Future precipitation has been modeled for the broad Hawaiian Islands and more specifically, Maui, to understand how climate and groundwater resources will be affected.

### **Geologic Setting and Hydrologic Connectivity**

Initial mapping by Stearns and MacDonald (1942) identified three distinct volcanic series in the region: Hāna Volcanics, Kula Volcanics, and Honomanū Basalt. While these series are composed of similar materials, basalts, lava, cinders, and typical extrusive volcanic rock, they represent different eruptive periods and stretches of time punctuated each of them, allowing soil layers and weathered surfaces to form in between the different layers. The Hāna Volcanics, occupying a small part of the eastern study area, are the smallest, most recent, and are highly permeable (Gingerich, 1999a). The Kula Volcanics erupted after the Honomanū series and covered much of northeast Maui's surface. They are theorized to hold perched groundwater and nearly cover the entirety of the lower Honomanū Basalt (Langenheim and Clague, 1987). This sprawling volcanic layer is hypothesized to be less permeable than the Honomanū Basalt due to a higher density from an increased quantity of silica sheets in the structure (Stearns and McDonald, 1942). The Honomanu Basalt is assumed to have a higher hydraulic conductivity relative to the Kula Volcanics (Gingerich, 1999a).

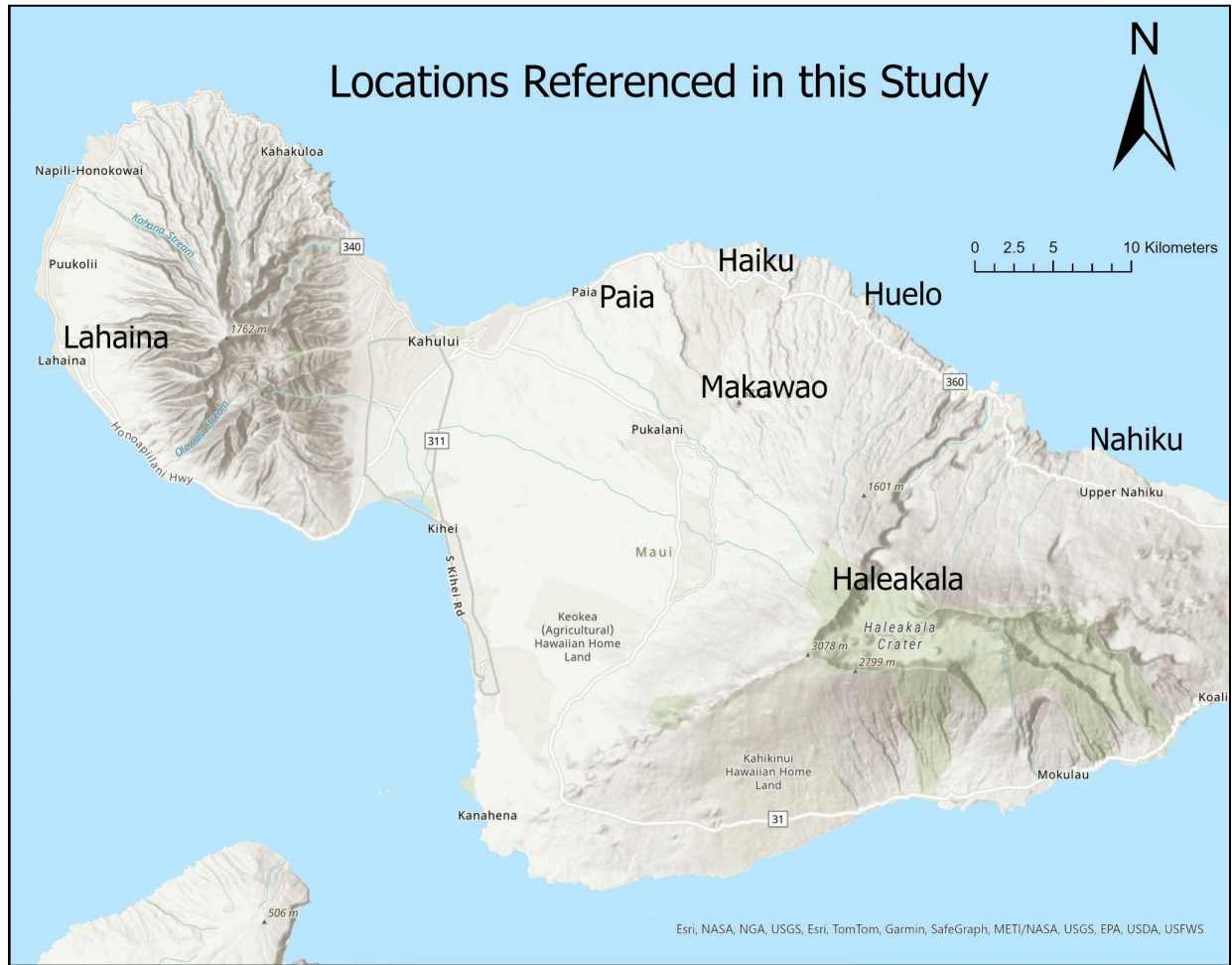


**Figure 1:** Locations mentioned within this study to familiarize the reader.

Because there was likely a long enough stretch of time between the Honomanu and Kula series for extensive weathering and thick soil layers to form on the now buried surface of the Honomanu lavas, the contact between these two volcanic series was hypothesized by Gingerich (1999b) to be an aquitard, thereby resisting flow, and creating a saturated zone above and an unsaturated zone below. Meyer (2000) countered this theory for the more easterly Nahiku area at least, where he theorized the existence of water bodies in both the Hana Volcanics, Kula Volcanics and the Honomanu Basalt, that conformed to fully-saturated conditions. The hydrologic differences between the two areas may be attributed to larger amounts of rainfall within the Nahiku area or possibly heterogeneity in the geology between

these areas (Meyer, 2000). Figure 1 provides a map of the area with streams, ditches, and geological units.

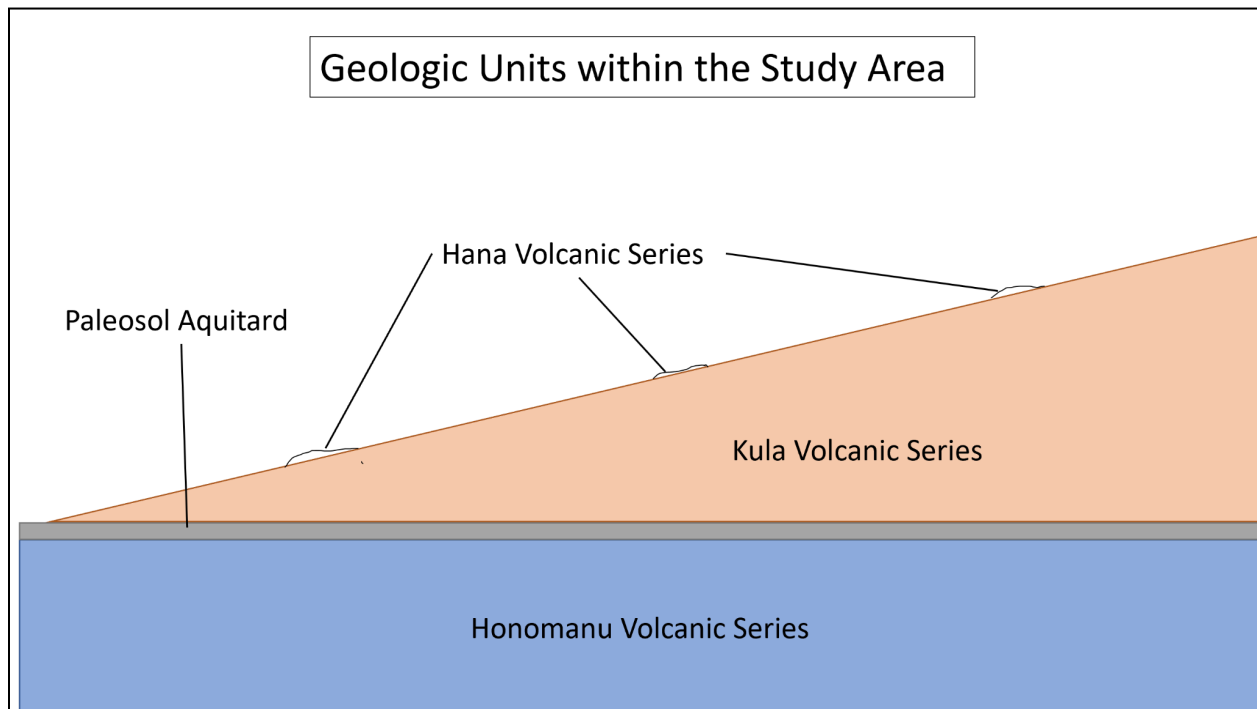


**Figure 2:** Conceptual model of geologic units within the study area.

The Honomanū Basalt is the foundation of the shield volcano and only outcrops near the coastline and in heavily eroded gulches (Stearns and McDonald, 1942) (see above in Figure 2). The differing permeabilities of Kula and Honomanu Basalts result in streams over Kula Volcanics usually leading to the ocean, while those over Honomanu Basalt typically drying up before reaching the coast (Scholl et al., 2002).

## II. Perched Groundwater Characteristics

Perched groundwater, considered young and not a viable long-term source according to Niu et al. (2020), was initially associated with the Kula Volcanics series (Gingerich, 1999a). Contrary to Niu et al. (2020), studies in Nāhiku propose perched aquifers present in all units, with faster recharge rates than previously assumed (Meyer, 2000). There is even a claim of a

community member with a shallow well at high elevation near Awalau Stream who lives autonomously using a well that likely taps into a perched water reservoir.

## VII. Hypotheses and Objectives

### **Hypotheses:**

1. Stream base flow is controlled by a perched aquifer and wells are fed by the basal aquifer, leaving an unsaturated space separating the two aquifers.
2. Future groundwater development will impact private wells through significant lowering of the water table, limiting residents' ability to withdraw groundwater.
3. The Ha'ikū and Huelo regions will experience a reduction in available groundwater recharge due to anticipated decreases in precipitation.

### **Objectives:**

1. Evaluate water quality from streams and existing wells by employing freshwater stable isotope content and major ion concentration analysis to determine if surface water and groundwater wells are both fed by a geochemically contiguous groundwater body.
2. Utilizing an established groundwater model for the study area, incorporate new hypothetical pumping scenarios with various numbers of municipal wells placed in plausible locations to quantify estimates of drawdown at private wells.
3. Perform an analysis of historical observed precipitation and recharge. Additionally, analyze future climate projections specific to Hawaii to produce a clear picture of historical precipitation trends and projected rainfall within Ha'ikū and Huelo.

## Methods

### I. Sample Collection and Lab Analysis

Water quality samples were collected at multiple locations and in some cases repeatedly at the same location throughout the study period. Specifically, eight sample locations (five

precipitation collection stations, two streams, and two wells) were sampled for water isotopes on a monthly basis for a period of 16 months. These samples are herein referred to as the monthly sample set. Other streams, wells, and springs were sampled opportunistically, some more than once and some only one time. These samples are herein referred to as the opportunistic sample set.

Five main water types were sampled during this study, wells, streams, springs, streambed seepage, and precipitation. Sampling locations were chosen based on location and availability due to many of the sampling sites being located on private property. Stream and spring sample sites were identified by connecting with community members who granted access. Spring and seepage samples were taken as close to the location where they exited the ground as possible.

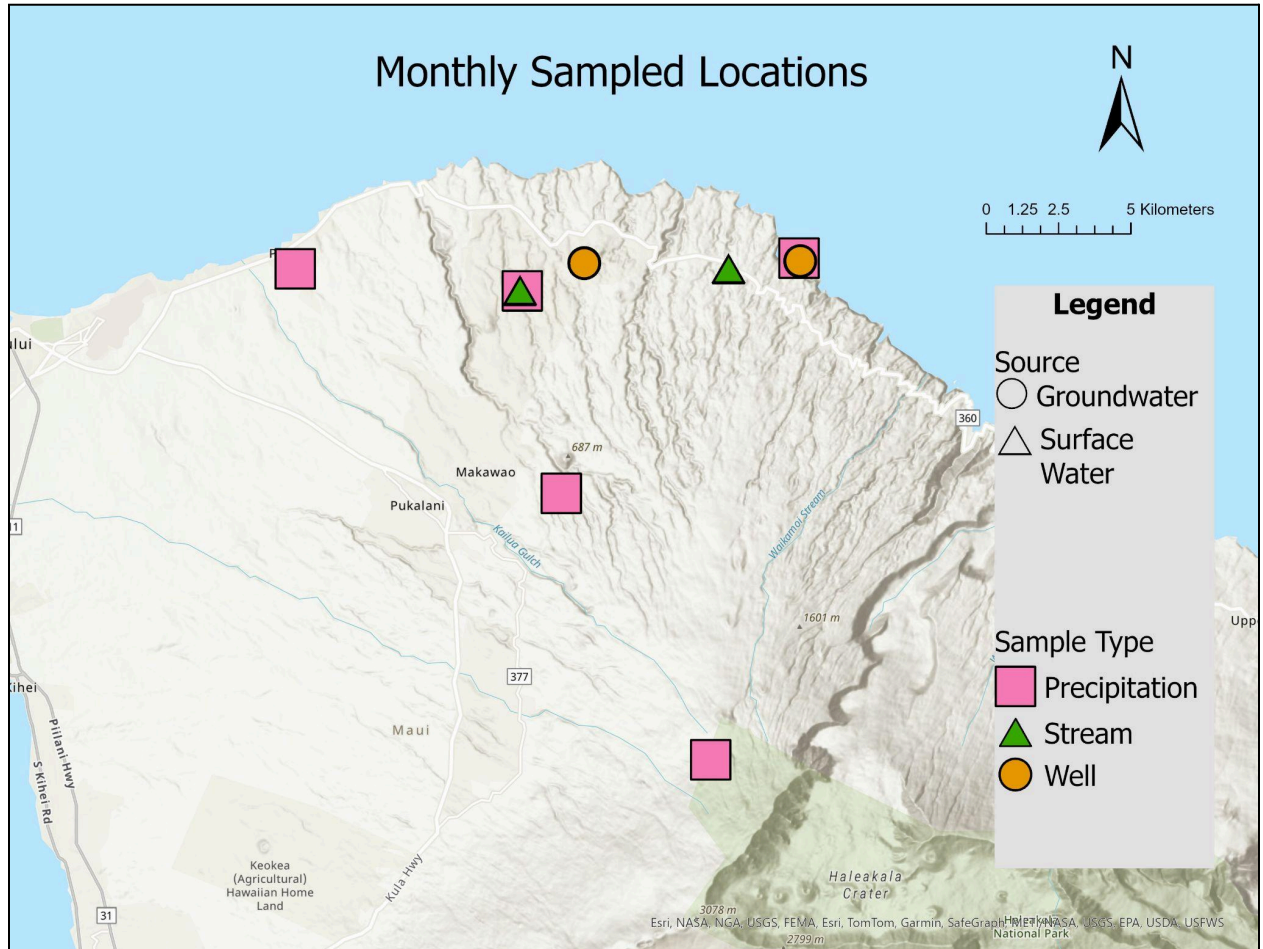


**Figure 3:** Locations that were sampled monthly throughout the study period.

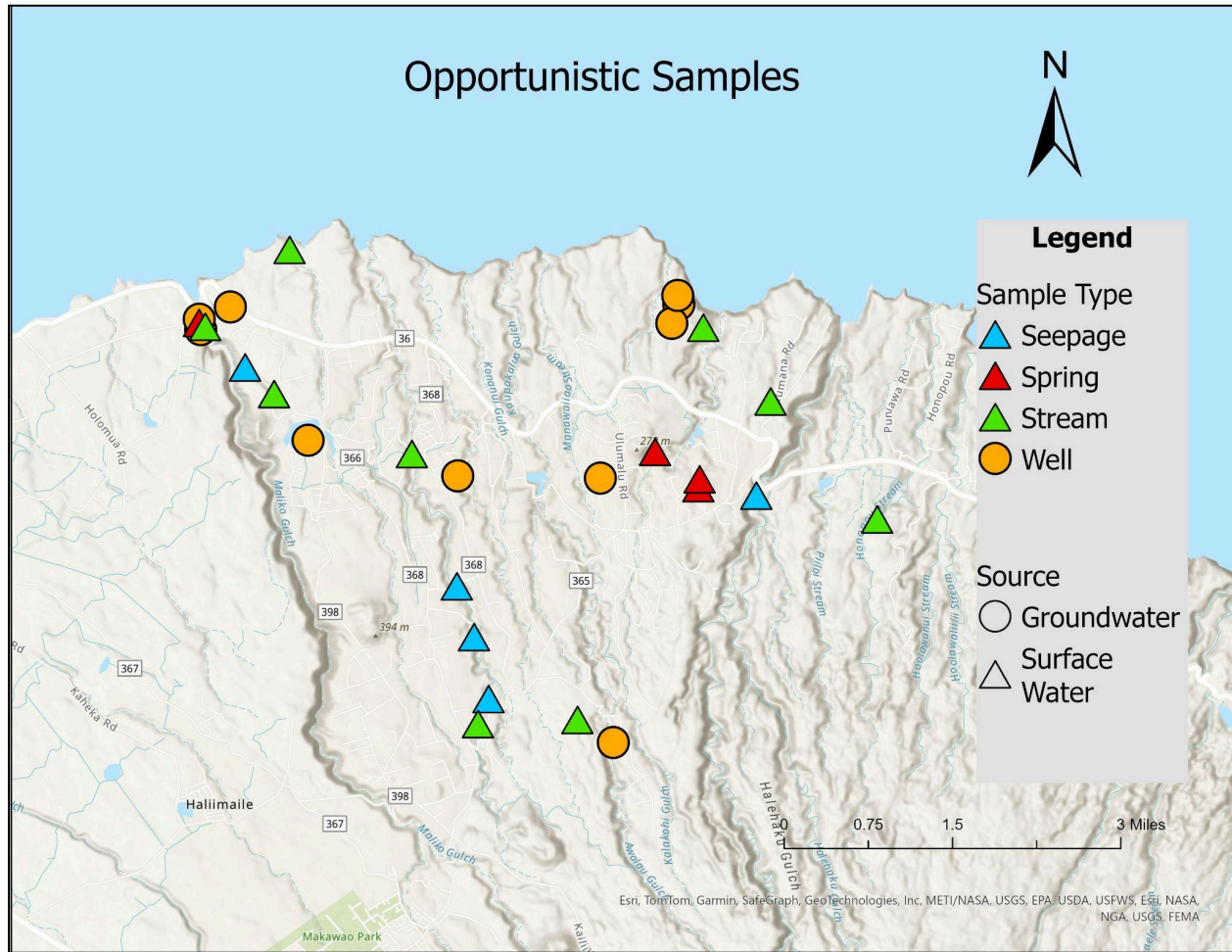


**Figure 4:** These sampled locations were not sampled monthly due to time constraints, access, or availability of homeowners.

At each location, one 20 mL glass bottle with a maximum headspace of two millimeters was collected for analysis of stable freshwater isotopic compositions of deuterium (D) and oxygen-18 ( $^{18}\text{O}$ ), and at some of the opportunistic locations a second bottle was collected for major ion analysis (see Figure 4). Water isotope samples (unfiltered) were collected in new 20 ml glass vials once the vial was triple rinsed with sample water. Unfiltered well samples were either collected from well sampling taps, well tanks, or household taps after water had been left to run for two minutes in order to collect freshly pumped water from wells. Isotope samples were stored at room temperature until they were analyzed at the University of Hawai‘i

Isotope Biogeochemistry Lab. Isotope samples were processed using a Picarro mass spectrometer.

Major ions were also collected in 60 mL triple rinsed HDPE plastic bottles. In order to prohibit bacteria within the water affecting the water quality parameters, 0.45  $\mu\text{m}$  nylon filters were used when collecting water samples for major ion analysis. Filtered well samples were also collected from the tap after water had been left to run for two minutes in order to collect freshly pumped water from wells. For major ion samples, basic water quality parameters were also recorded including: temperature, dissolved oxygen, conductivity, salinity and pH using a multiparameter water quality sensor (manufactured by Yellow Springs Instrument YSI). Ion samples were transferred into a freezer for storage until analysis. Major ion samples were analyzed at the University of Hawai'i Water Resources Research Lab using a Dual Dionex Aquion Ion Chromatographs, AS-DV Autosampler at the WRRC Environmental Chemistry Lab, following established protocols (Révész and Coplen, 2008a, Révész and Coplen, 2008b).



**Figure 5:** A precipitation collector on Haleakalā located near the Haleakalā visitor center at 2,125 m above mean sea level.

Five precipitation collection stations were deployed in Ha‘ikū, Paia, Makawao, Huelo, and near the visitor station of Haleakalā National Park (see Figure 3). Precipitation collection stations were placed to create two separate transects, one across the altitude gradient from Ha‘ikū to Haleakalā, and one to capture an East-West gradient from Huelo to Paia, in order to capture coastal and altitude variation. Precipitation collection stations were fabricated using 5-gallon buckets following a modified design by Scholl et al. (2002) (see Figure 5). Collectors were topped with buchner funnels to prevent large debris from entering. Stands were constructed to immobilize the collectors and keep the funnels level, and tape was replaced each month as an extra precaution. 16 oz. of fresh mineral oil was added to each collector when deployed and also when redeployed each month to minimize water evaporation (Scholl et al., 1996).

Precipitation collection stations were sampled monthly. Sampling was performed by pouring the contents of the collector into a larger bucket with a spigot. Once the mineral oil

and water had separated after two minutes, an unfiltered isotope sample was taken using the spigot after allowing roughly 20 mL of water to flow, clearing the spigot of any debris that could contaminate the sample. The rest of the water was measured using a graduated cylinder and the monthly volume was recorded at each station. Precipitation quantity measurements were compared with precipitation isotope data to observe rainy and dry season trends.

## II. Historical Precipitation Record

The Hawaii Rainfall Atlas uses historical data to indicate that the study area has a steep average-annual rainfall gradient that reaches up to 5000 mm in the higher elevation areas and up to 2000 mm in the coastal areas (Giambelluca et al., 2013). There is also the presence of an east-west gradient in precipitation that increases eastward. There are conflicting predictions as to what will happen to Hawaii's precipitation in the future. Hawaii will likely experience complex microclimatic shifts that will occur on each island (DeMaagd & Roberts, 2021).

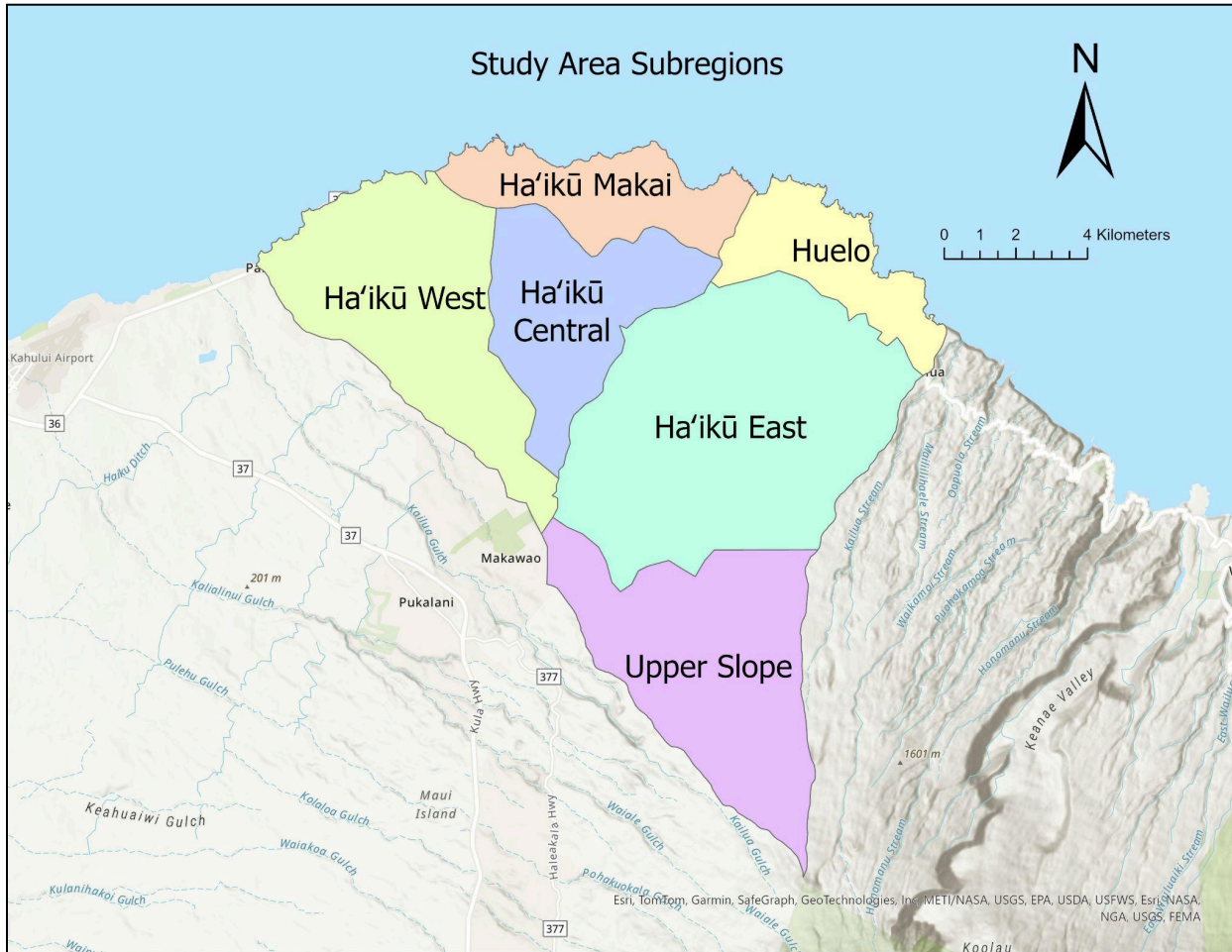


**Figure 6:** The study area was divided into six subregions for precipitation analysis.

We conducted a review of historical rainfall data to understand historical trends and the effects of ENSO on the region’s precipitation. The area was divided into six different subregions to be able to communicate variation within the study area. These subregions were named Ha’ikū Makai, Ha’ikū Central, Ha’ikū East, Ha’ikū West, Huelo, and Upper Ha’ikū in Figure 6.

Precipitation data from the Hawaii Climate Data Portal by Longman et al. (n.d.) was used in conjunction with a script created by Longman et al. (2023) to create a climate change, variability, and drought (CCVD) portfolios for each subregion. Recorded sea surface temperature changes were used to calculate ENSO phases from the NOAA National Weather

Service Climate (n.d.). We used data containing El Niño and La Niña years from the Golden Gate Weather Services (Null, 2024) to compare rain gauge data released by Huang et al. (2022) in csv format from four stations to visualize the effects of ENSO. We downloaded data from the stations set up by Huang et al. that were located within the study area to analyze the historical rainfall and its fluctuations (2022). The data was resampled to yearly totals within a period of consistent data availability between all four stations.

### III. Groundwater Modeling Methods

We used a MODFLOW based groundwater model by Whittier and El-Kadi (2014). We obtained the MODFLOW model files to use in this study for the explicit purpose of simulating the freshwater lens. Streams were not included in this model under the assumption that the groundwater is not connected to the surface water present in the streams. The nutrient transport components of the model were not utilized. Although the model was fairly limited in its application, it was calibrated by El-Kadi with existing observation data at wells specifically to be able to accurately simulate for water table elevations, thus we determined that it was an applicable model to repurpose for this study with no modifications to the base-case model needed.

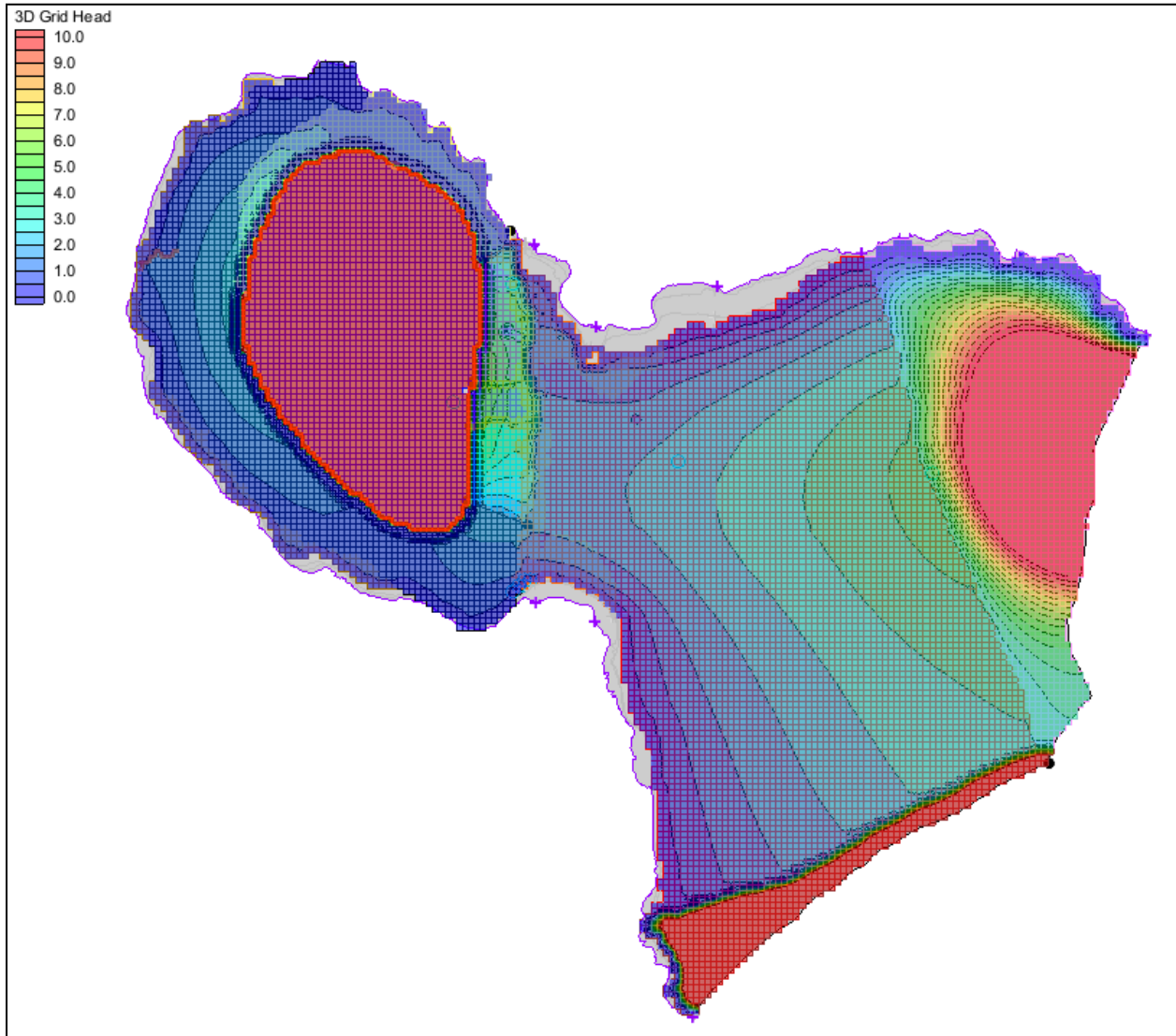


**Figure 7:** Modeled base case water table map for most of Maui (Whittier and El-Kadi, 2014).

This groundwater model contains four layers, a grid of 122,304 cells of the same size, and two values for hydraulic conductivity, vertical and horizontal (see Figure 7). The horizontal hydraulic conductivity is set to zero which indicates no horizontal flow or impermeability in the horizontal direction. The vertical hydraulic conductivity is set to 100 m/d. The cell size is in XYZ format in meters and is 325x277.5x1,000. The recharge rate varies within the model from 0-2.63 m/yr.

The model was applied to represent hypothetical future well pumping scenarios in northeastern Maui. Hypothetical municipal wells were placed at reasonable sites and three existing well locations were used as monitoring points to simulate the drawdown effect on well heads in different pumpage scenarios. The criteria for potential future municipal well development describes the max scenario as 10 hypothetical wells pumping at one million gallons per day situated at an elevation of 305 meters in the Maui Island Water Use & Development Plan. The three pumping rates were chosen as 33%, 66% and 100% of the maximum pumping rate of one million gallons per day. The hypothetical modeled well locations were chosen by identifying county or state owned lands present at an elevation near the 305 meters contour line, and could be reasonable places to develop a well.

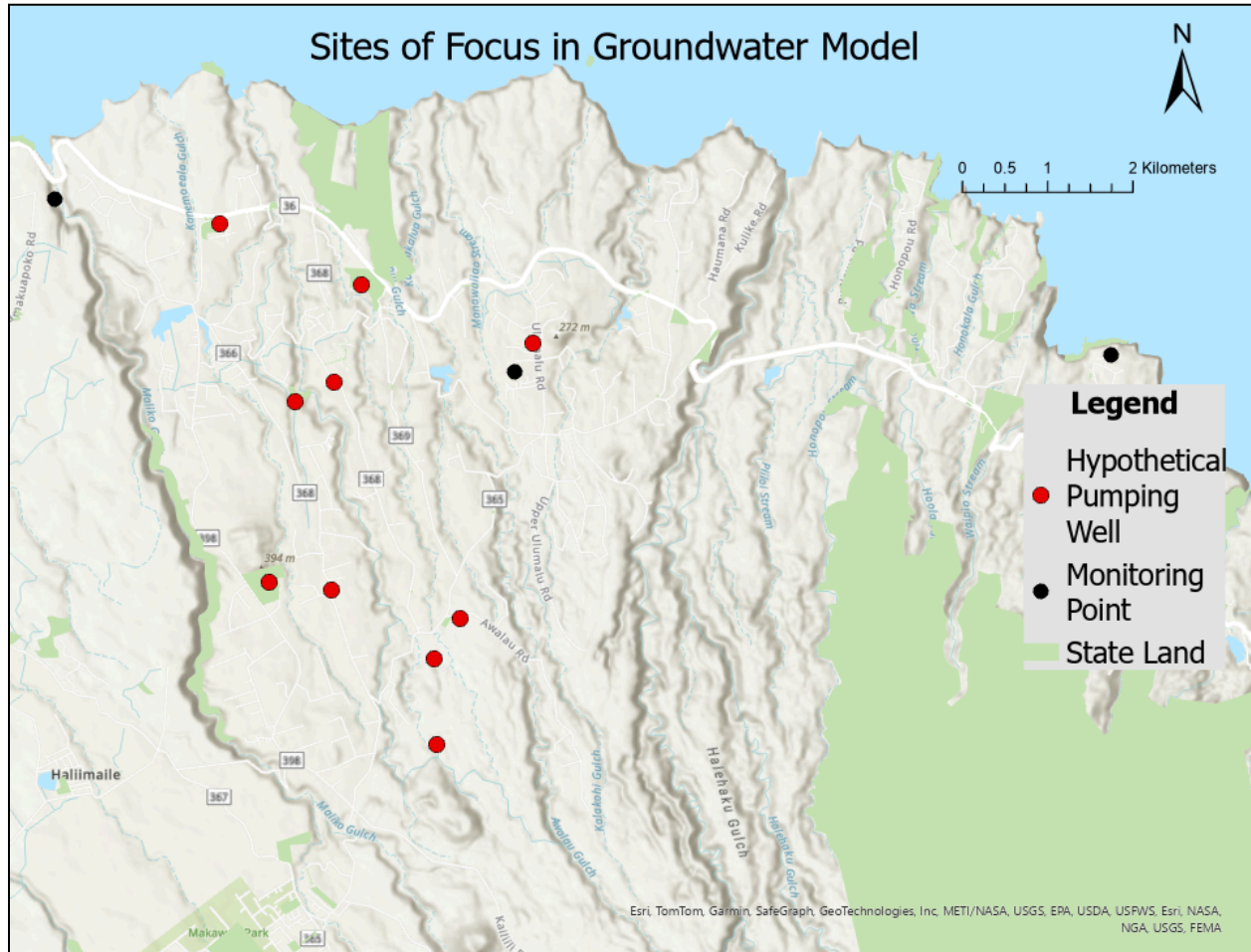


**Figure 8:** Locations of monitoring points and hypothetical pumping wells. Hypothetical pumping wells are each located on Maui County and state land according to a parcels layer downloaded from from the Hawaii Statewide GIS Program (2022).

The monitoring points represent three existing privately owned, active wells (see Figure 8). Pumpage varies in each scenario between 100%, 66%, and 33%, of the specified maximum of 1 million gallons per day. Note that due to assumed small pumping rates and unknown quantities, pumping rates for private wells are not included in the model.

# Results

## I. Potential Hydraulic Connections

### A. Precipitation

#### Precipitation Isotopes Volumetric, $^{18}\text{O}$ Content and Temporal Variability

There are large fluctuations in  $^{18}\text{O}$  at each of the collector stations even within each season. For instance, the precipitation collection station at Ha'ikū, located in the north of the subregion Ha'ikū Central, shows monthly precipitation variability between 0-680+ mm during the rainy season, peaking mid-season (see Figure 1).

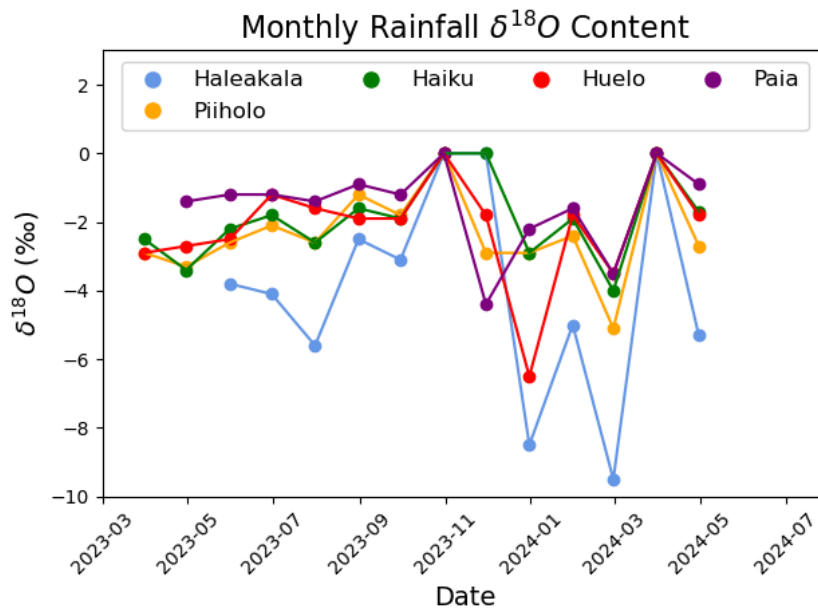


**Figure 9:** Monthly rainfall  $\delta^{18}\text{O}$  and  $\delta^2\text{H}$  values over time at precipitation collectors. Each color represents an individual precipitation collection station from 03/2023 - 07/2023.

Paia consistently had the smallest rainfall volume throughout the sampling period while Haleakalā received the greatest amount (see Figure 9). Elevation clearly played a role in rainfall volume during this study period.

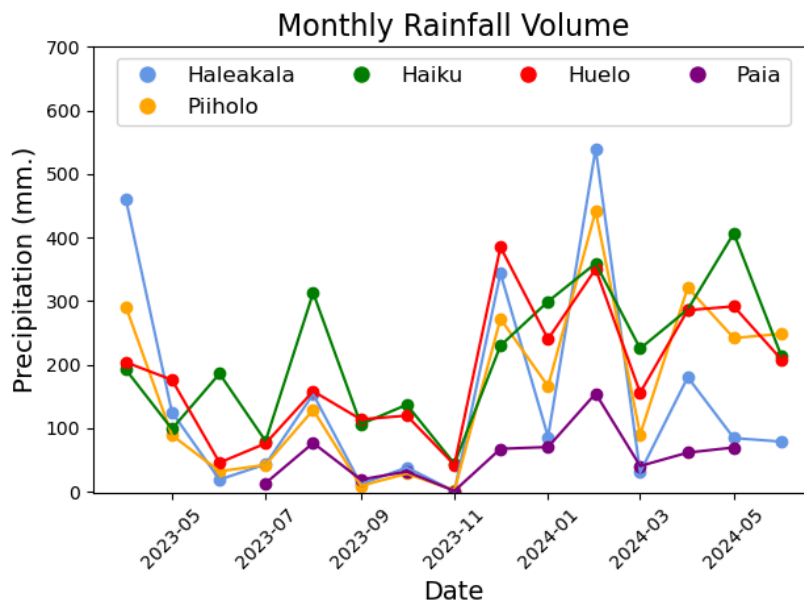


**Figure 10:** Monthly rainfall volume over time. Each color represents an individual precipitation collection station from 03/2023 - 07/2023.

The rainy season appears to coincide with precipitation more negative in both  $\delta^{18}\text{O}$  and  $\delta^2\text{H}$  content (see Figure 10). More isotopic variability is present in the rainy season than in the dry season. One limitation in the collection of precipitation samples is that some samples did not yield data some months due to several reasons: not all precipitation collection stations were installed at the same time, mishandling of samples during transport, and feline fecal contamination within a collector.

## B. Precipitation Isotope Content

A range of isotope values are seen at each location. Paia bears the maximum  $\delta^{18}\text{O}$  value and Haleakalā bears the minimum  $\delta^{18}\text{O}$  value. The largest and smallest ranges of isotope values locations are the same as the maximum and minimum values.

**Table 1:** Summary table of isotope values for each location.

Location	Haleakalā	Haiku	Huelo	Piiholo	Paia
Max $\delta^{18}\text{O}$ (‰)	-2.5	-1.5	-1.2	-1.2	-0.5
Max $\delta^2\text{H}$ (‰)	-11.2	8.5	9.4	6.2	13.9
Min $\delta^{18}\text{O}$ (‰)	-8.5	-3.4	-6.5	-3.4	-4.4
Min $\delta^2\text{H}$ (‰)	-55	-17.4	-38.7	-17.5	-26
Mean $\delta^{18}\text{O}$ (‰)	-4.6	-2.2	-2.2	-2.6	-1.6
Mean $\delta^2\text{H}$ (‰)	-24	-2.5	-2.8	-6.3	-1.8
Range $\delta^{18}\text{O}$ (‰)	6	1.9	5.3	2.2	3.9
Range $\delta^2\text{H}$ (‰)	43.8	25.9	48.1	23.7	39.9

Coastal and slightly inland precipitation exhibited the most enriched  $\delta^{18}\text{O}$  and  $\delta^2\text{H}$  content, whereas precipitation near the peak of Haleakalā had the most depleted values (see Table 1). Altitude clearly plays a role in the water isotope content of precipitation as the isotopic values become more depleted with elevation gain (see Table 1). East-west geographic change also seems to have an effect to a lesser extent as seen in the relationship between the Paia and Huelo precipitation collection stations (see Figure 9). These two stations were located at similar altitudes on opposite sides of the study area and Paia showed a more enriched  $\delta^{18}\text{O}$  content than Huelo.

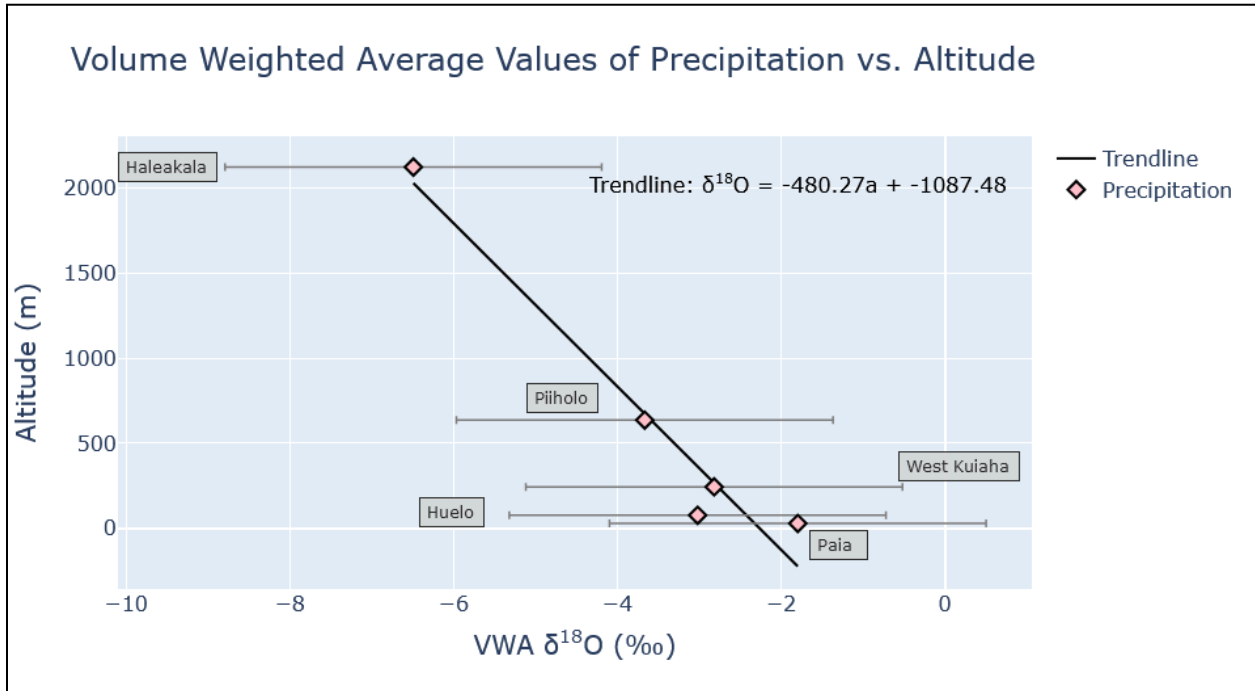


**Figure 11:** Precipitation sample volume weighted average (VWA)  $\delta^{18}\text{O}$  values compared to precipitation collection station elevation in meters. Error bars for each station represent the standard deviation calculated when averaging the isotopic content at each unique location.

Volume weighted averages were calculated by multiplying the monthly  $\delta^{18}\text{O}$  value by its volume in mL (see Figure 11). Each result was then added and divided by the sum of the volume to produce the volume weighted average. Volume weighted average calculations were based on Tachera (2022) who examined the hydrogeochemistry of west Hawaii's Water Cycle. This calculation was performed because it captures both the variations in precipitation volume and isotope values as it varies during the study period.

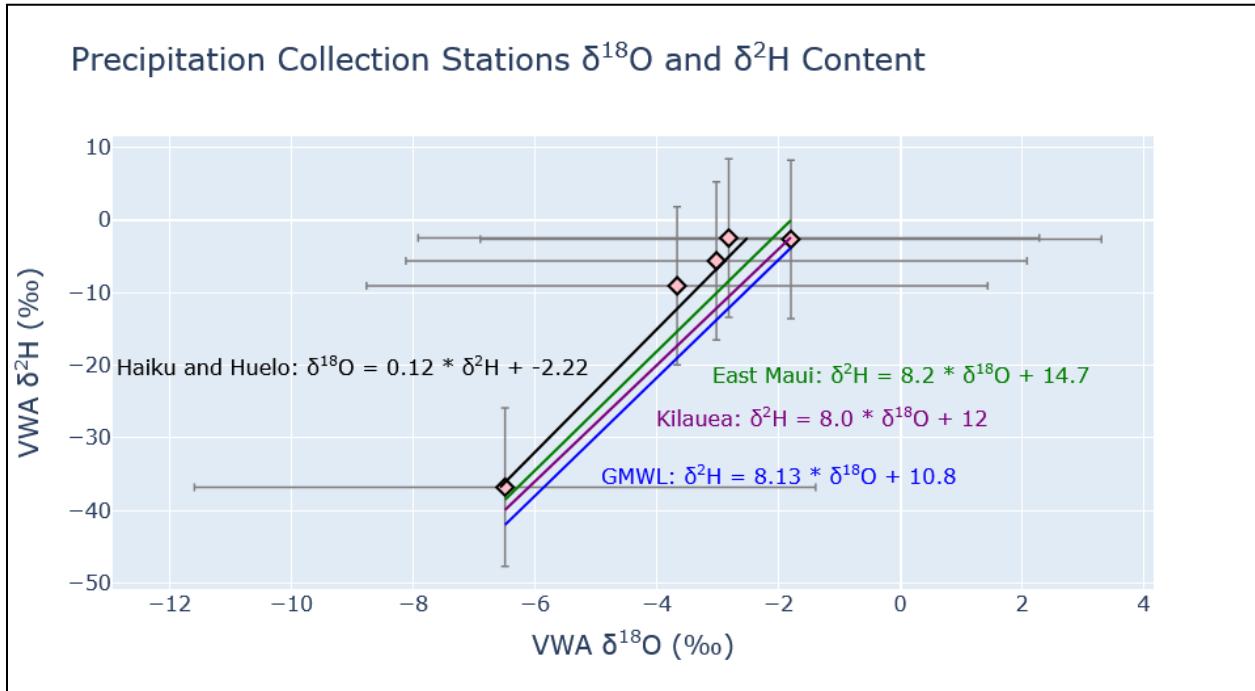


**Figure 12:** Precipitation volume weighted averages of  $\delta^{18}\text{O}$  values are plotted against corresponding volume weighted averages of  $\delta^2\text{H}$  values (Figure). Each point (diamonds) represents a volume weighted average from each precipitation sampler in this study highlighting regional differences across this relatively small area. Each of the colored lines represents a meteoric water line (MWL), or a best fit line of the data pertaining to a specific area. The green line represents the Scholl et al. (2002) MWL for eastern Maui, the purple line represents the Scholl et al. (1996) Kilauea Volcano on Hawaii Island, and the blue line represents the Global MWL. The black line that represents data from this study in Ha'ikū and Huelo shows that the water samples here are much more enriched, which may be attributed to increased rainfall. Error bars for each station represent the standard deviation calculated when averaging the isotopic content at each unique location.

Comparing all of the isotope values between precipitation and terrestrial freshwater samples can provide insights into the recharge source of terrestrial waters. Our observed data show that precipitation has the widest range and streams and springs have the smallest range of the isotope results (see Figure 12). Precipitation, namely one of the monthly samples from

Haleakalā shows the most depleted isotope content (see Figure 12). Different storms can yield different isotope values based on their mechanism of condensation and cloud height altitude (Dorres et al., 2020).

Previously reported global and local meteoric water lines (MWLs) plotted on Figure 10 are less enriched in both  $\delta^{18}\text{O}$  and  $\delta^2\text{H}$  than the study area's values. The color of each trendline equation corresponds to the respective MWL. The MWL for eastern Maui by Scholl et al. (2002) is only slightly lower than that of our data for northeast Maui. This may be due to the southeastern part of Maui including a drier area, which can lead to more evaporation, and in turn more fractionation, making the Scholl et al. (2002) MWL plot below the northeast Maui MWL. The Scholl et al. (1996) MWL for Kilauea, a volcano on Hawaii Island, plots even lower. This difference might be attributed to a latitudinal shift or a drier part of Hawaii Island. The Global Meteoric Water Line (GMWL) is the lowest in the plot because it is an average derived from rain water composition around the world not accounting for local conditions and rain pattern variations.

Streams also have multiple noticeable outliers. The stream sample that is the most isotopically depleted is a sample from Twin Falls Stream in Huelo, one of the monthly samples that bears an isotopic range of values that experienced small fluctuations throughout the study. Springs and seepage show a very small range and show little fluctuation. One limitation of some of the well samples is that some were taken directly from storage tanks to which the well pumped and stored water. Another limitation is that the samples were collected by hand from a spigot and not directly from the source.

## Terrestrial Samples

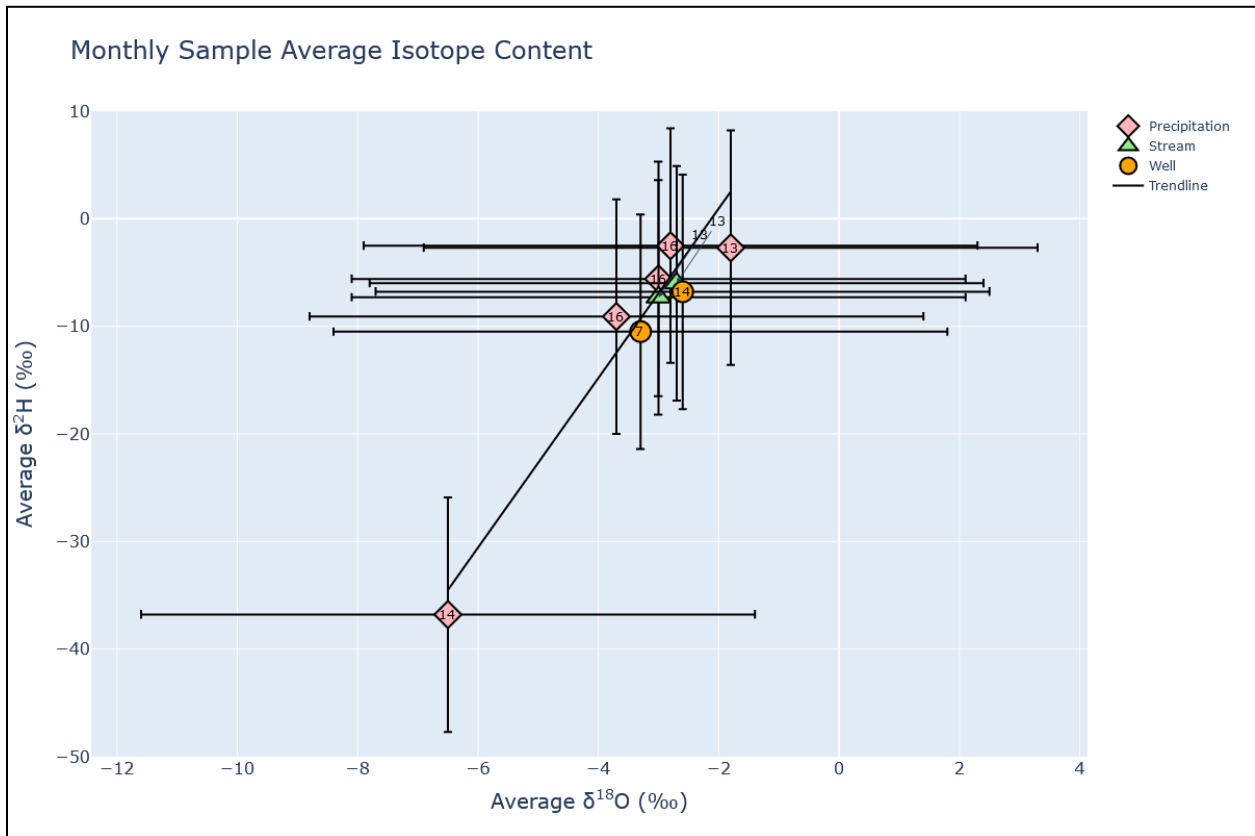


**Figure 13:** Monthly sample average  $\delta^{18}\text{O}$  values versus  $\delta^2\text{H}$  values for individual streams and wells. Precipitation markers represent the volume weighted average isotopic content of individual precipitation collection stations. Error bars show the standard deviation of the mean. The number within the marker or line pointing to the marker represents the number of monthly samples that were taken at each site.

The precipitation in the monthly samples occupy the widest range of isotope values (see Figure 13). Wells vary less than precipitation, but streams vary the least (see Figure 13). The largest outlier is Haleakalā as seen on previous figures. Most of the precipitation appears to have a higher ratio of  $\delta^2\text{H}$  values to  $\delta^{18}\text{O}$  values than the streams and wells.

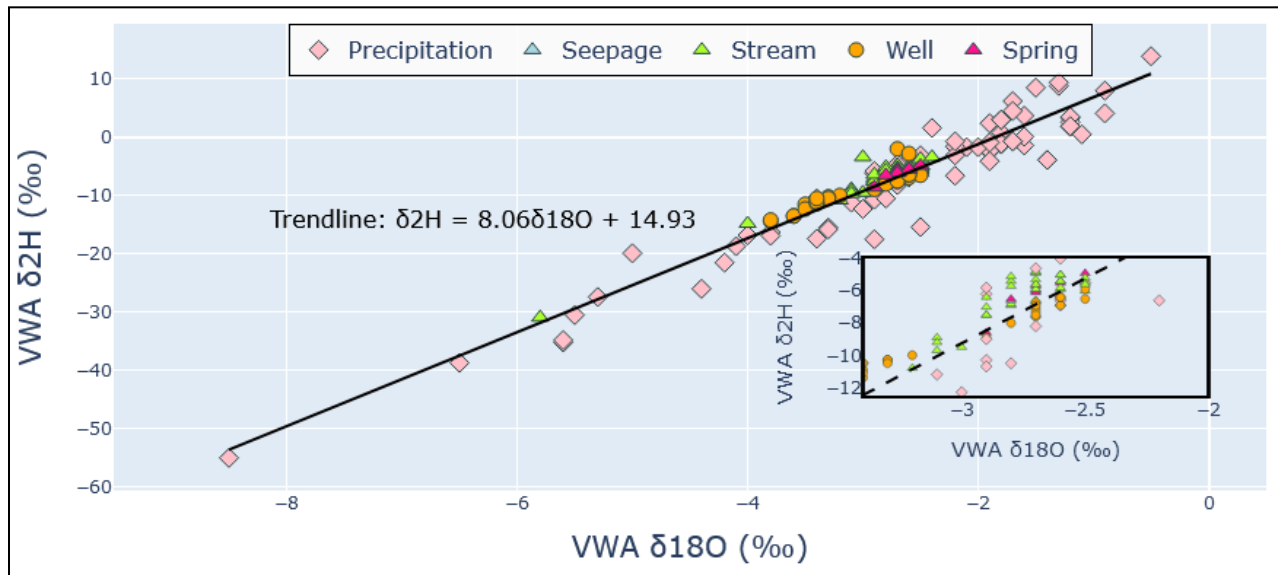


**Figure 14:** All monthly and opportunistic water isotope samples with an inset plot to better view the center cluster.

Each water source occupies a different range of isotope values highlighting the unique average (see Figure 14). Sample isotope value range decreases as one moves from precipitation to surface water (streams and springs) and finally to wells. There is some overlap between streams and springs, but there is very little between springs and wells.

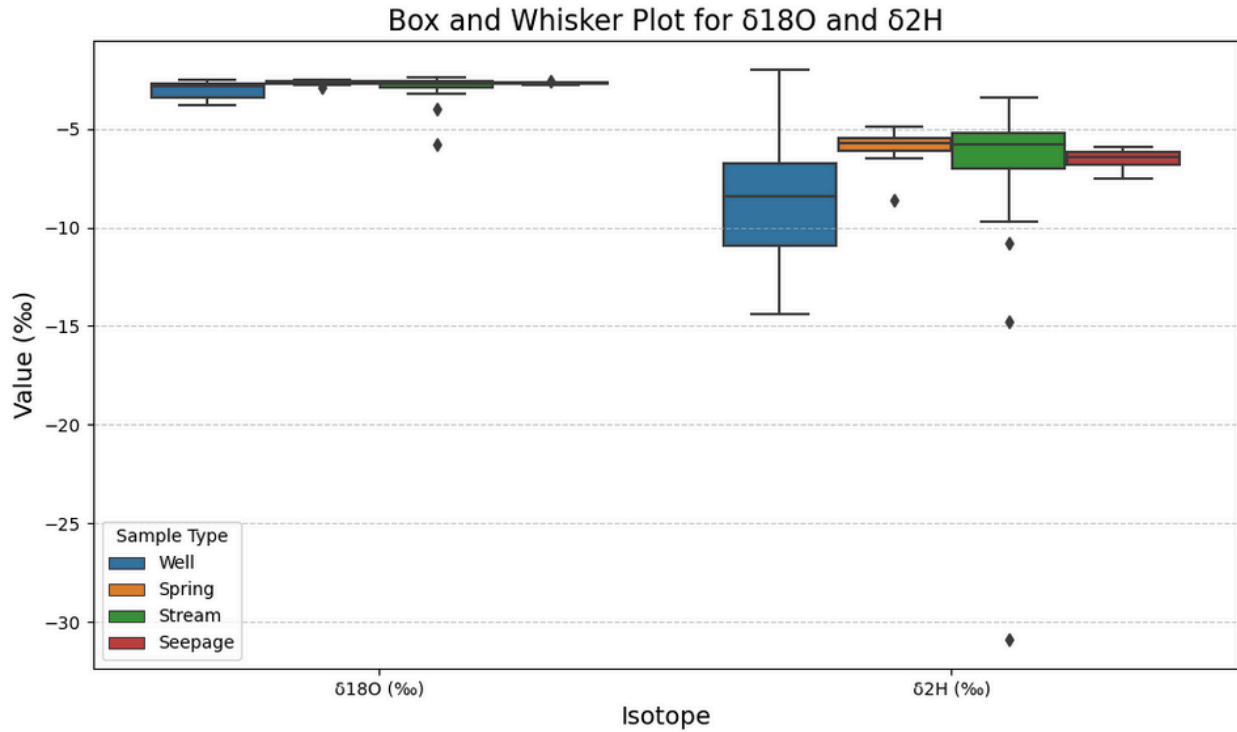


**Figure 15:** Water isotope  $\delta^2\text{H}$  boxplots for all samples of different types including wells, streams, springs, and seepage.

$\delta^2\text{H}$  values of water sources show much greater variation than  $\delta^{18}\text{O}$  values. There is much greater variation in wells and streams than in springs and seepage for both sampled isotopes (see Figure 15). Springs and seepage show the least variation in both sampled isotopes. The greatest outliers are present in the  $\delta^2\text{H}$  wells values.

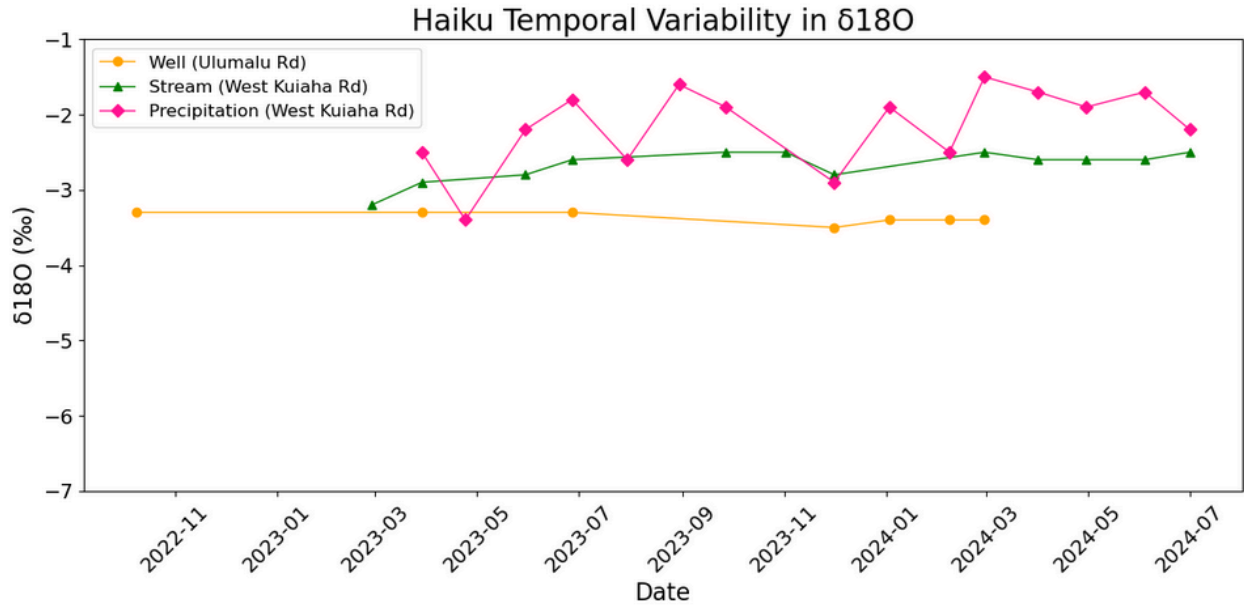
**Table 2:** Table showing the minimum, maximum, mean, and range of  $\delta^{18}\text{O}$  and  $\delta^2\text{H}$  values for seepage, springs, streams, and wells.

<b>Sample Type</b>	<b><math>\delta^{18}\text{O}</math> Min</b>	<b><math>\delta^{18}\text{O}</math> Max</b>	<b><math>\delta^{18}\text{O}</math> Mean</b>	<b><math>\delta^{18}\text{O}</math> Range</b>	<b><math>\delta^2\text{H}</math> Min</b>	<b><math>\delta^2\text{H}</math> Max</b>	<b><math>\delta^2\text{H}</math> Mean</b>	<b><math>\delta^2\text{H}</math> Range</b>
Seepage	-2.8	-2.6	-2.7	0.2	-7.5	-5.9	-6.6	1.6
Spring	-2.9	-2.5	-2.7	0.4	-8.6	-4.9	-6.0	3.7
Stream	-5.8	-2.4	-2.9	3.4	-30.9	-3.4	-7.1	27.5
Well	-3.8	-2.5	-3.0	1.3	-14.4	-2	-8.9	12.4

The maximum  $\delta^{18}\text{O}$  values are present in the streams. The minimum  $\delta^{18}\text{O}$  values are present in the seepage. There is much greater variation present in the  $\delta^{18}\text{O}$  values than the  $\delta^2\text{H}$  values (see Table 2).

C. Monthly Repeated Samples

a.



b.

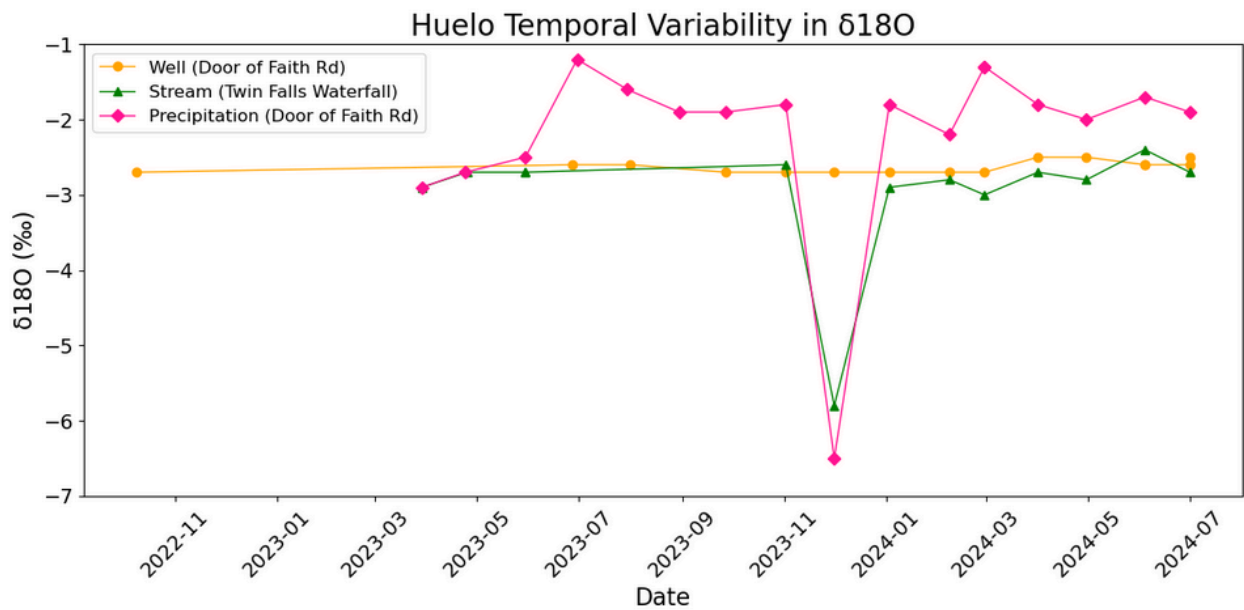


**Figure 16a & b:** Comparison of geochemical signatures of an individual well and stream in Ha‘ikū and Huelo.

A well, stream, and spring each within Ha'ikū and Huelo were selected for repeated sampling during the study period to compare the differences between water sources in the west (Ha'ikū) and east (Huelo) regions of the study area. The well in Huelo appears to be distinctly different from the well in Ha'ikū (see Figure 16a & b). The opposite is true for streams which bear similar isotopic content, but follow very different patterns. Precipitation shows the most fluctuation in both Ha'ikū and Huelo (see Figure 16a & b). Streams show less variability than precipitation and wells show the least variability. This data is limited by the fact that there are only two continuous sources of data in each location.

## D. Similarities and Differences of Major Ions

### Major Ion Crossplot

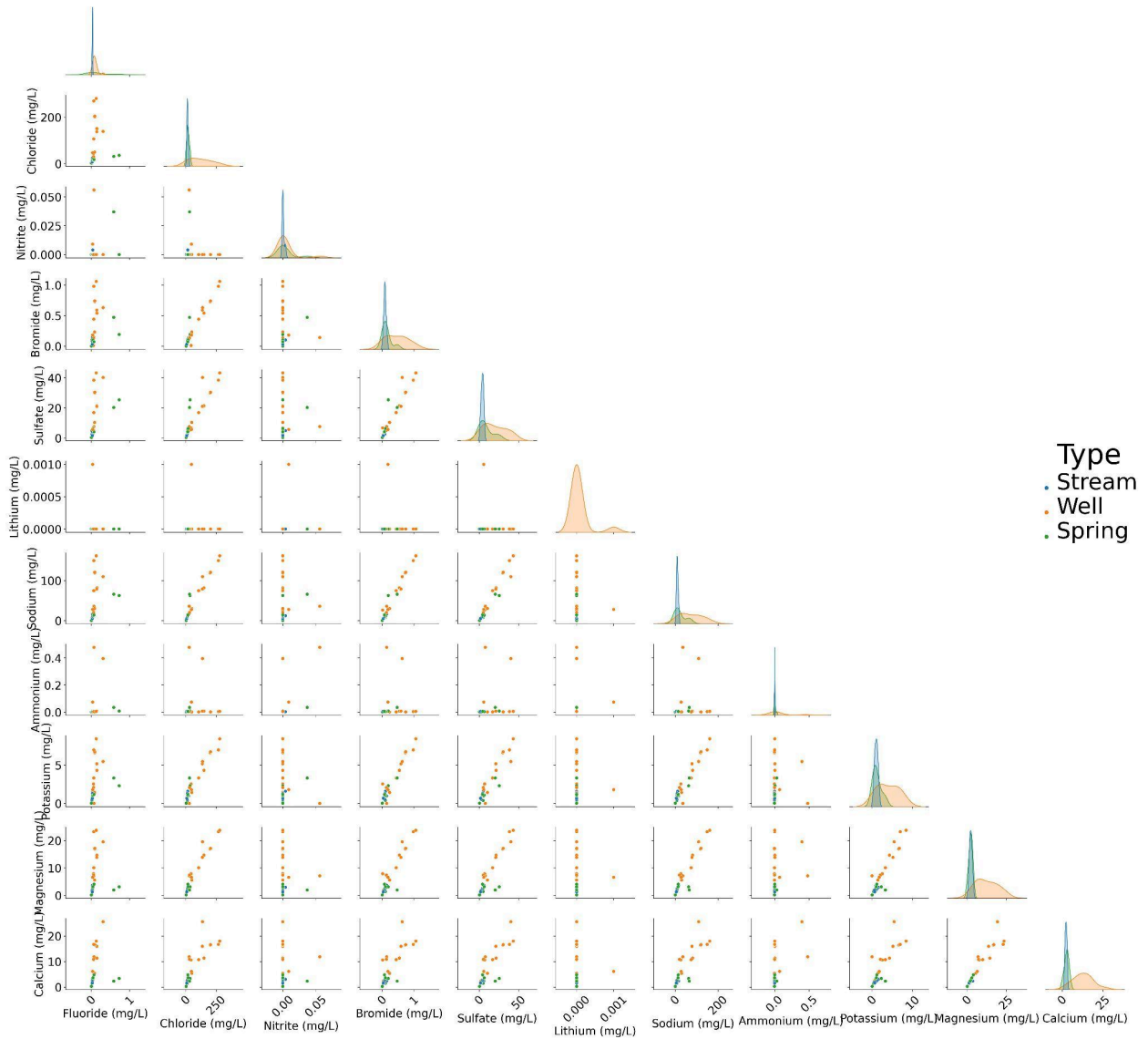


**Figure 17:** Major ion matrix plot of major ions. Plots in the middle where the same ion is present on both the x and y axis show sample distribution. 8a shows mostly clear linear trends in major ions. 8b & 8c show mostly less clear linear trends in ions.

Major ion concentrations including sodium, chloride, potassium, bromide, and nitrate are plotted against one other to compare the streams, springs, and wells. Similarly to the

isotopes, wells plot separate from surface water samples, further suggesting that surface water and basal water are separate entities. The largest ion concentration found is chloride within the wells possibly due to proximity to the coast, causing brackish saltwater intrusion, and thus an increase in salinity. It is unlikely that an increase in other major ions is apparent in locations closer to the coast. The ratios of ions within seawater and fresh groundwater present themselves differently due to the dissolution of rock. Wells overall have much higher concentrations of all ions than streams and springs (see Figure 17). The cause of this can be attributed to interactions between the water and volcanic rock as it flows. Many of the ions share a strong correlation. The stream and spring samples tend to have higher concentrations of ions than wells, potentially suggesting that surface water carries higher concentrations than groundwater. Major ions in springs and streams show a narrow distribution. Groundwater shows a wider, sometimes even binomial distribution (Fig. 16). Some springs also have binomial distribution but still not as wide as wells.

#### E. Results of Analysis of Stable Isotopes and Major Ions

In this statistical analysis, wells are considered groundwater and streams, springs, and seeps are considered surface water. Creating two groups based on this categorization allowed for comparison in statistical analysis in the following section. We used unpaired t-tests to compare the  $^{18}\text{O}$  and the  $^2\text{H}$  values of the distinct groups that are mentioned to determine if the groundwater and surface water have similar values. Lescesen et al. used multiple statistical analyses, including unpaired t-tests for independent samples to compare water quality parameters and found that the differences between individual parameters were statistically significant, meaning that the freshwater resources had the potential for development along the border of western Serbia (2004).

**Table 3a & b:** Statistical results from unpaired T-tests between surface water (springs and streams) and groundwater (wells) in both Ha‘ikū and Huelo. Ions were not divided by area and represent the entire study area due to the lack of samples collected in Huelo.

a.

Location	Isotope	t-Statistic	p-Value	Significance
Ha‘ikū	<sup>18</sup> O	-4.46	8.11E-05	Yes
Ha‘ikū	<sup>2</sup> H	-3.77	6.81E-04	Yes
Huelo	<sup>18</sup> O	1.44	1.71E-01	No
Huelo	<sup>2</sup> H	0.44	6.65E-01	No

b.

Ion	t-Statistic	p-Value	Significance
Fluoride	0.36	0.72	No
Chloride	-4.26	0	Yes
Nitrite	-0.36	0.72	No
Bromide	-3.56	0	Yes
Nitrate	0.03	0.98	No
Sulfate	-3.12	0.01	Yes
Magnesium	-5.48	0	Yes
Calcium	-6.29	0	Yes

The following table shows the significance results of two unpaired t-tests that compare the mean ion concentrations of well samples to the mean ion concentrations of springs and streams within Ha‘ikū and Huelo. The results do not show a statistically significant difference between the surface water and groundwater in Ha‘ikū or between the two in Huelo (see Table 3a & b).

The isotope results do show a statistically significant difference between the surface water and the groundwater of each respective region. According to the p-values of the unpaired

t-tests within Ha‘ikū, the statistical difference suggests that surface water may not originate from the same source as groundwater. Statistical analysis within Huelo suggests that surface water and groundwater may originate from the same source. In Huelo, it is likely that the surface water and groundwater may be well mixed and part of a continuous aquifer body, based on the two sampling groupings potentially being statistically different. The ions were chosen to represent the study area as a whole because few major ion samples were collected within Huelo. Most of the ions suggest that groundwater and surface water originate from different sources, though some do not show conclusive patterns. Nitrite concentrations in samples were almost entirely below the method detection limit of 19.5 parts per billion (ppb), therefore the small available sample size made an unpaired T-test unable to yield a useful result.

### Stream and Well Water Level Comparison

Many of the coastal and eastern wells and streams have much lower overall water level elevations. There appears to be a gradual shift to higher well head and stream elevations with increases in elevation and eastward movement.

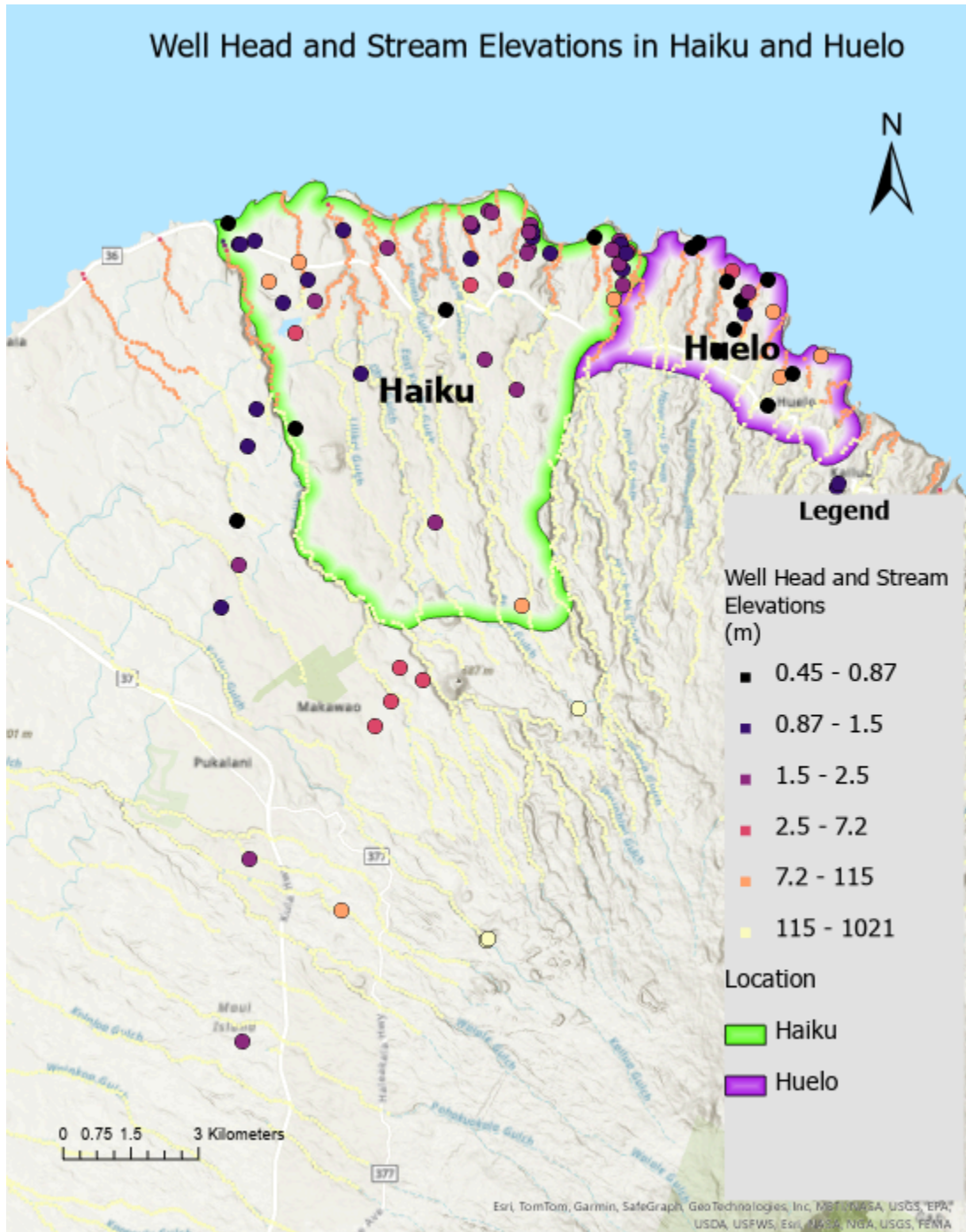


**Figure 18:** Well head measurements (larger circles) from State Commission on Water Resources Management (CWRM) well records and stream elevations (smaller squares) extracted as land surface elevation from a high resolution digital elevation model. Elevation and well head units are recorded as above mean sea level (amsl).

Farther geographic movement eastward towards Huelo shows more varied well heads and stream elevations within smaller geographic areas than in the western part of the study area near Haiku (see Figure 18). Wells present a much greater range in well head than streams do in elevation.

## Limitations

Saltwater intrusion was considered as a potential factor that can affect the isotope content of the data, therefore the effects of isotopic mixing of ocean water (with a known salt content) were estimated using an equation developed by Hunt and Rosa (2009). We wanted to determine if saltwater intrusion had a measurable effect on isotope values. The saltwater unmixing calculations suggested that ocean water mixing had a negligible effect on groundwater isotope values. Since it appears that seawater mixing has a negligible effect on major ion or water isotope concentrations, the results presented here utilize unmixed concentration values. The groundwater well head measurements are based on records from different years, meaning that the well head measurements may have changed over time.

## II. Groundwater Model and Future Scenarios

### A. Groundwater Scenario Results

Groundwater modeling scenarios showed a wide range of modeled drawdown rates in water table elevation that varied based on the number of future wells placed and their pumping rate. The multiple scenarios allow for an understanding of how water availability can change in response to increased groundwater withdrawals.

**Table 4:** MODFLOW results. A total of 16 different scenarios were run to observe changes in monitoring point heads. The pumping rate units are in million gallons per day (MGD).

Scenario	Number of Wells	Pumping Rate for each well (MGD)	Monitoring Point 1 (% change)	Monitoring Point 2 (% change)	Monitoring Point 3 (% change)
Base Case	0	0	Original head: 7.42 m	Original head: 2.50 m	Original head: 1.92 m
1	10	1	-13.2	-1.7	-1.1
2	10	0.67	-11.1	-2.9	-3.0
3	10	0.33	-6.0	-1.4	-1.5
4	8	1	-13.6	-3.6	-3.7
5	8	0.67	-9.0	-2.4	-2.5
6	8	0.33	-4.5	-1.2	-1.2
7	6	1	-6.6	-2.3	-2.9
8	6	0.67	-4.4	-1.6	-1.9
9	6	0.33	-2.2	-0.8	-1.0
10	4	1	-3.2	-1.8	-2.2
11	4	0.67	-2.1	-1.2	-1.4
12	4	0.33	-1.1	-0.6	-0.7
13	2	1	-1.6	-0.9	-1.1
14	2	0.67	-1.0	-0.6	-0.7
15	2	0.33	-0.5	-0.3	-0.4

According to the model results, the water levels at monitoring points are likely to experience a decrease under any number of wells and pumping rate tested (see Table 4). The maximum scenario of introducing 10 wells pumping 1 MGD decreased the water level by more than 13% in monitoring point 1. This monitoring point experienced the greatest decrease by almost one meter. There is no uniform decrease in water levels within the monitoring points.

This can likely be attributed to the geometry of the hypothetical well placement and the locations of monitoring points.

It should be noted that this model only simulates the basal aquifer under the assumption that perched aquifer(s) are hydraulically disconnected from the basal aquifer. Streams were not represented because of the assumption declared in Objective 1 that the streams are not hydraulically connected to the groundwater. This is supported by the significance of the p-test results that may suggest that streams do not feed into the wells in the study area.

## Limitations

Utilizing Whittier and El-Kadi's model has some limitations that must be acknowledged in the results. There are several limitations within this model; the well data is from 2022, only the basal aquifer is simulated, and few wells had publicly available well depth and pumpage rates available to act as monitoring points. Saltwater is not simulated because of the results of the saltwater unmixing calculations. The hypothetical future wells that were placed may not be the real locations of the wells when and if they are drilled. An underreporting or lack of reporting of well pumping rates may underestimate the current total rate of pumping. Most recent well pumpage from three private wells that were also sampled for isotopes were included in the model. Access to a larger sample size of private water sources, especially wells, would improve the models calibration and thus representativeness of model results.

## III. Precipitation Analysis

### A. Historical Precipitation and Trends in Subregions

Many members of the community have reported noticing changes in rainfall within the last 50 years. Understanding how local precipitation has varied over time offers a comparison between one's memories and historical data. Rainfall data from the Hawaii Climate Data Portal from 1920-2024 was used to understand the significance of historical trends (Longman et al., n.d.). All six subregions show similar precipitation records over the past 100 years. One subregion plot, Haiku Central, was chosen to be presented in this study as it was considered

that it best captured all aspects of the surrounding subregions based on its geographical position.

### Rainfall Trend 1920- 2024 : Central

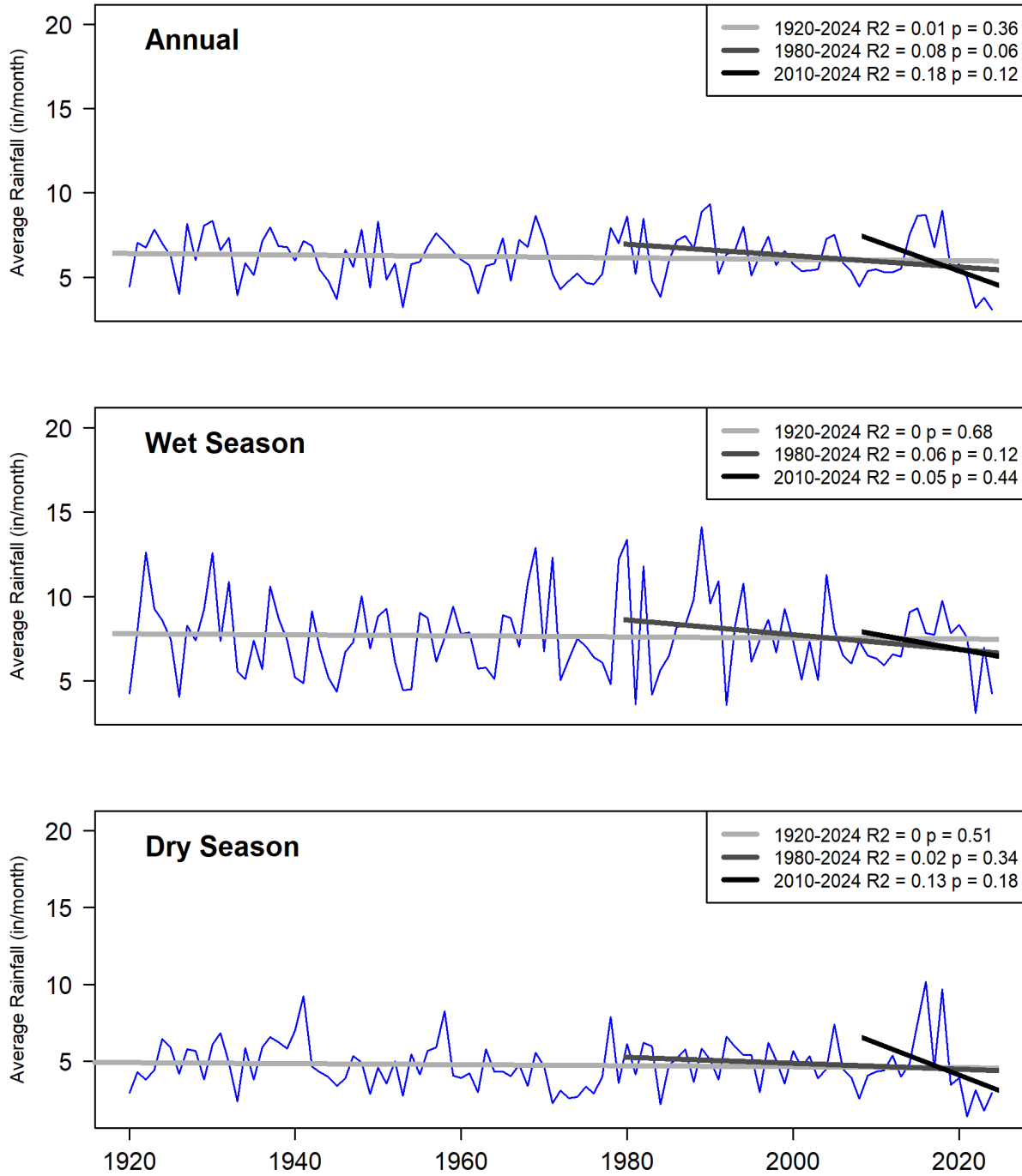


**Figure 19:** Annual average monthly precipitation in Central Ha'ikū with trends during three periods. Precipitation data is from the Hawaii Climate Data Portal by Longman et al. (n.d.) and script is by Longman et al. (2023).

**Table 5:** Trend analysis results of each subregion for three different time periods. Precipitation data is from the Hawaii Climate Data Portal by Longman et al. (n.d.) and script is by Longman et al. (2023).

<b>Location</b>	<b>Period</b>	<b>Trend</b>	<b>P-value</b>
West Ha‘ikū	1920 - 2024	Decrease	0.33
West Ha‘ikū	1980 - 2024	Decrease	0.02
West Ha‘ikū	2010 - 2024	Decrease	0.16
East Ha‘ikū	1920 - 2024	Decrease	0.01
East Ha‘ikū	1980 - 2024	Decrease	0.03
East Ha‘ikū	2010 - 2024	Decrease	0.38
Ha‘ikū Makai	1920 - 2024	Decrease	0.17
Ha‘ikū Makai	1980 - 2024	Decrease	0.03
Ha‘ikū Makai	2010 - 2024	Decrease	0.14
Central	1920 - 2024	Decrease	0.36
Central	1980 - 2024	Decrease	0.06
Central	2010 - 2024	Decrease	0.12
Huelo	1920 - 2024	Decrease	0.01
Huelo	1980 - 2024	Decrease	0.04
Huelo	2010 - 2024	Decrease	0.28

Upper Slope	1920 - 2024	Decrease	0.13
Upper Slope	1980 - 2024	Decrease	0.03
Upper Slope	2010 - 2024	Increase	0.80

Nearly all six subregions including Ha‘ikū East, Ha‘ikū Makai, West Ha‘ikū, Huelo, Central, and Upper Slope show a decrease in all three historical rainfall trends between 1920-2024 (see Table 5). The exception is the Upper Slope which shows an increasing trend in precipitation during 2010-2024 (see Figure 19). It must be noted that this trend bears a p-value of 0.8, making it not a significant trend. Many of the trends do not bear any significance due to their p-values being greater than 0.05.

The analysis indicates that precipitation in the study area has experienced a near uniform decrease in precipitation since 1920, but the lack of significance does limit how confidently we can say that these trends in rainfall are not just due to significant rainfall variability in understanding how precipitation has been affected within the past century. The limitations of this data are station locations and the accuracy of the data. Interpolation was performed by Longman et al. to fill gaps (n.d.). Longman et al. performed a 20-year precipitation analysis to understand the future of large scale weather events in Hawaii (2021). According to one study by Longman et al., precipitation data gaps were interpolated using a product that can access all observational data in a grid format to produce 25-year sets of gridded rainfall maps of specific areas (Longman et al., 2021). It is likely that Longman et al. performed a similar interpolation with the above data.

## B. Local Precipitation Variation with ENSO

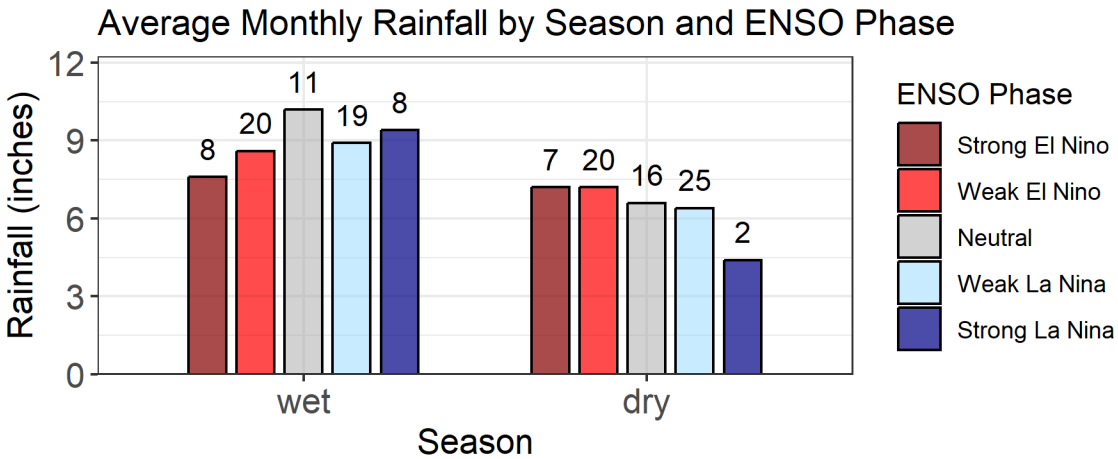


**Figure 20:** Bar Plot of average monthly rainfall grouped by season and ENSO phase for the Central Haiku subregion. Numbers above the bars are how many seasons from 1950 to 2024 fell within each ENSO phase.

The wet season shows a noticeable increase in precipitation when compared to the dry season, as would be expected (see Figure 20). Shifts in ENSO may cause further precipitation changes in each season. In the wet season, strong La Niña events correlate with generally higher rainfall, then during strong El Niño events, which correlate with lower amounts of rainfall (see Figure 20). The available data appear to show the opposite during the dry season where strong La Niña events correlate with lower precipitation and vice versa for dry seasons. These seasonal shifts that correlate with ENSO cycles are not uniform. In the wet season, the neutral state of ENSO shows a higher quantity of rainfall than the strong La Niña. In the dry season, the weak El Niño shows a higher quantity of rainfall than the strong El Niño. This data is limited by the amount of individually recorded ENSO phases.

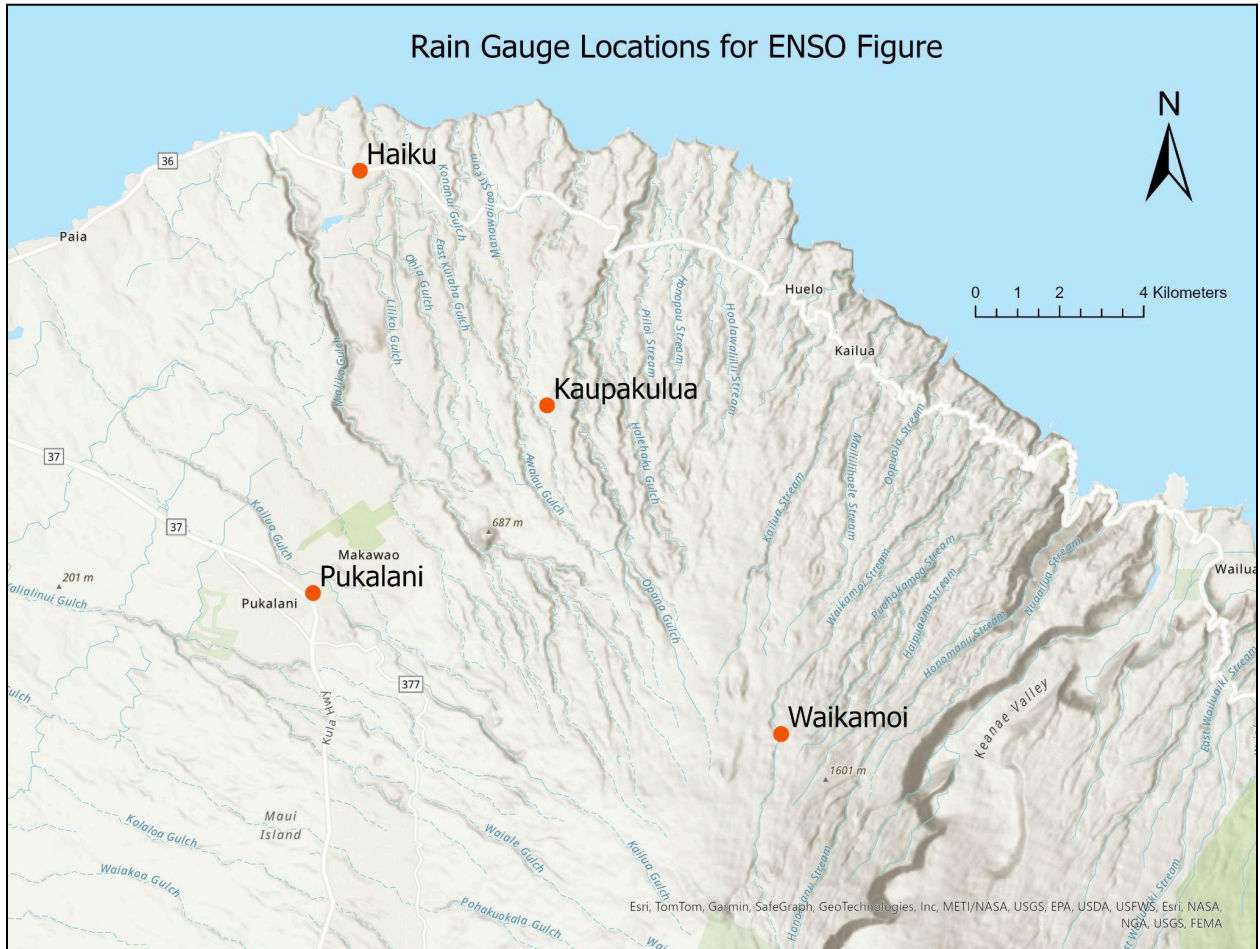


**Figure 21:** Locations of rain gauge data displayed in next figure.

Four long-term rain gauges from a data release by Huang et al. present in the study area were analyzed for their potential relationship with ENSO (2022). The locations of these four rain gauges are displayed above in and around the study area of Haiku and Huelo (see Figure 21).

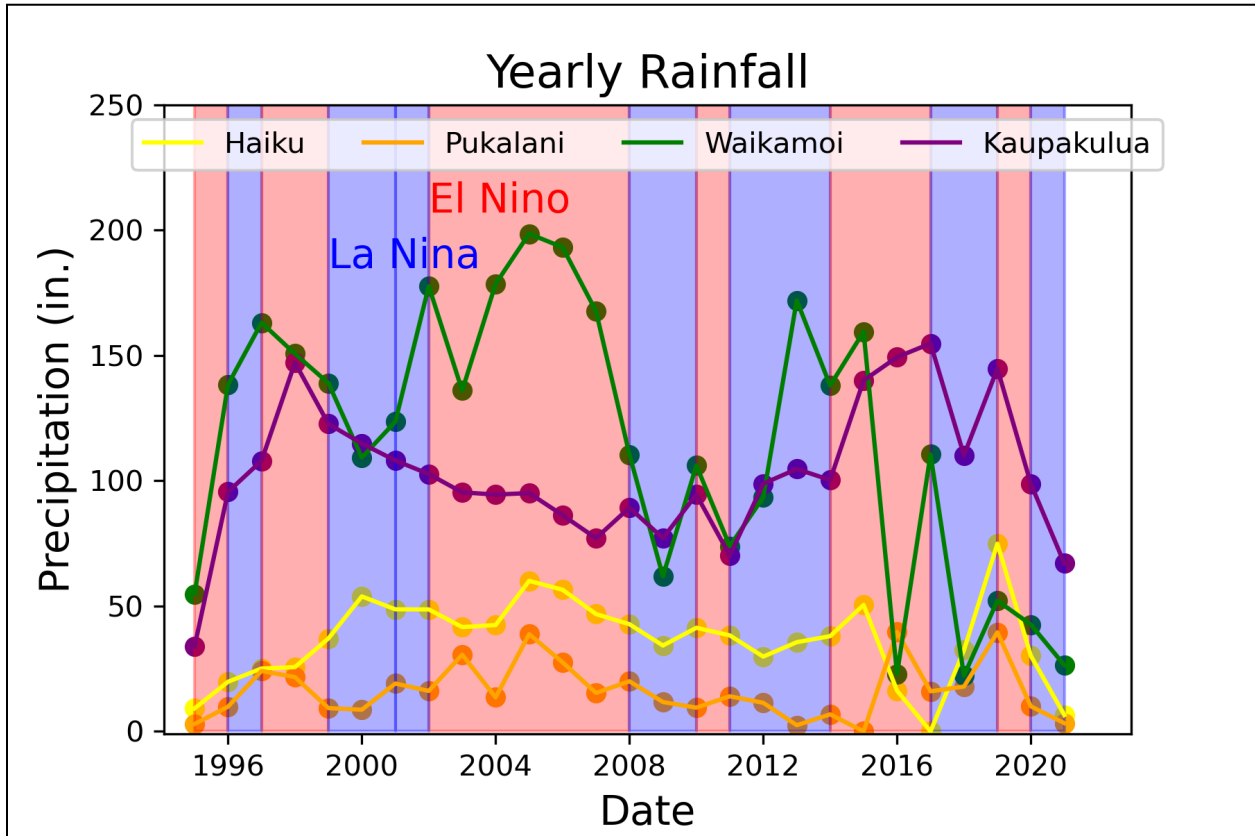


**Figure 22:** Annual rainfall at four rain stations, plotted alongside each El Niño and La Niña. Precipitation data is from Huang et al. (2022), aggregated to yearly values, and ENSO phase data is from Null (2024).

Over nearly 100 years, the study area has experienced highly variable rainfall Figure 19). Based on the analysis of rain gauge data from Huang et al. (2022), El Niño and La Niña do not have a clear and consistent impact on rainfall quantity of all of the rain gauge sites, however some patterns are visually recognizable (see Figure 22). Changes in rainfall at one station can be seen in other stations with varying degrees of change.

The analysis of annual precipitation data of the four stations was performed to assess the existence of patterns during both El Niño and La Niña years. We used paired t-tests for this analysis because the timeframe was shared. For each station, the total precipitation of each individual El Niño or La Niña event was compared to the respective average precipitation of

all El Niño or La Niña events between 1994-2022 in order to identify if patterns exist in ENSO. The appendix IV results include the p-values for both total and mean precipitation, along with labels indicating whether the event precipitation data for each year was significantly different ("D") from the whole or not ("N") from the average precipitation during the respective climatic event.

**Table 6:** Paired t-test results summarized into years that are statistically different and years that are not statistically different.

	Number of years that are Not statistically different than average rainfall	Number of years that are statistically different than average rainfall
El Niño	17	27
La Niña	29	34

The above table compares individual El Niño or La Niña events to their respective groups as a whole (see Table 6). The majority of the paired t-tests ran show that most individual ENSO events are statistically different and do not share a relationship with their average over the last 28 years.

### Future Precipitation Projections

Timm et al. (2015) applied statistical downscaling with the Coupled Model Intercomparison Phase 5 (CMIP5) global model for the major islands of Hawaii and produced two different scenarios, Representative Concentration Pathway (RCP) 4.5 and RCP8.5, that both predict a slight precipitation increase in the rainy season and decrease in the dry season in Northeastern Maui. Xue et al. (2020) used a dynamical climate modeling approach to develop contrasting results for much of the island of Maui, including Ha‘ikū, where projecting mean

rainfall to increase in both dry and wet seasons. With increased precipitation, groundwater recharge and streamflow would be assumed to increase as well for Northeastern Maui, but the mean precipitation and recharge of the Hawaiian archipelago is expected to decrease (Xue et al., 2020).

Brewington et al. (2019) created an integrated land cover/hydrological modeling framework with two future scenarios for Maui. RCP 8.5 and A1B applied future dry conditions and future wet conditions, respectively, but found similar results in that precipitation increased on the windward side of the island, but not the leeward (Brewington et al., 2019). Total precipitation was projected to increase for Maui (Brewington et al., 2019). These results agree with the earlier climate study that focused more broadly on the major Hawaiian Islands by Zhang et al. (2016). Zhang et al. (2016) used dynamical downscaling to produce a Hawaiian Regional Climate Model (HRCM) to simulate current and 2080-2099 future scenarios for the Hawaiian Islands. Leeward sides of the islands were found to have a decrease in clouds and rainfall and windward sides of the islands were found to have an increase in clouds and rainfall.

Previous water budgets have been made to understand the impacts of climate change on groundwater recharge and other water budget parameters. Shade (1999) created a water budget for the island of Maui and calculated the average precipitation and recharge volume to be 2,246 Mgal/d and 1,064 Mgal/d, respectively. Johnson et al. (2014) determined the recharge volume to be higher than Shade's calculation at 1,309 Mgal/d. Mair et al. (2019) developed a water budget model with three scenarios for Maui using 2017 historical land cover data: one current scenario and two future scenarios showing one wetter and one drier than current conditions. In order to show a range of changes in future climate, two high resolution downscaled climate projection datasets were chosen (Mair et al., 2019).

Rotzoll and Izuka (2020) created three water budgets and three numerical groundwater models calibrated in steady-state mode, simulating Maui and two other major Hawaiian Islands using the U.S. Geological Survey's (USGS) finite-difference groundwater-modeling program MODFLOW-2005 (Harbaugh, 2005). Most of the recharge on Maui was found to flow through caprock into the ocean (Rotzoll & Izuka, 2020). The areas that receive more

groundwater recharge than the rest of Maui will likely continue to receive more attention in the future as an exportable groundwater source for other parts of the island.

## Limitations

The main limitation of the historical precipitation analysis is the gaps that are present in the data due to technical issues. These were filled by their author's respective methods such as using grid observational data to interpolate data that was not collected. Gaps in precipitation data such as the 2016 Haiku rain gauge were filled in using ENSO data from Golden Gate Weather Services (Null, 2024).

## Discussion

Groundwater movement is largely influenced by the complex geologic setting on the northern flank of Haleakalā. The study area is characterized by volcanic dikes and transitions between volcanic series. The high hydraulic conductivity of the Honomanu Basalt contrasts with the lower conductivity of the Kula Volcanics, affecting how groundwater flows through different units. Understanding how these units play a role is imperative for predicting how vulnerable groundwater systems are to both natural and anthropogenic changes.

This hydrologic study of Ha'ikū and Huelo provides a detailed analysis of groundwater availability, geochemical signatures, and the impacts of future climate scenarios. Geochemical analyses through unpaired t-tests of stable isotope and major ion data indicate that surface water and groundwater are unlikely to share the same origin when considering the study area as a whole. When analyzed in smaller regions, a localized analysis shows significant variability. One theory is that there may not be as contiguous of low permeability perching layers, causing groundwater to have a similar isotopic content to that of surface water. In other words, surface water may be feeding into groundwater sources in Huelo as a result of higher hydraulic conductivity. There are many shallow wells in Huelo, suggesting that these may draw from perched aquifers that are fed by surface water, leading to similar signatures.

Precipitation and mixing of streams with differing isotope values may also be causing similar isotopic values within sources. Precipitation may be great enough to fully saturate the aquifer even if the hydrogeology is similar due to the higher amounts of rainfall found in Huelo.

According to our statistical analysis, wells are likely fed by the basal aquifer in Haiku. In Huelo, wells may also be fed by the streams in addition to the basal aquifer. We found several potential anomalies that support and contest the assumption that wells are recharged by solely the basal aquifer.



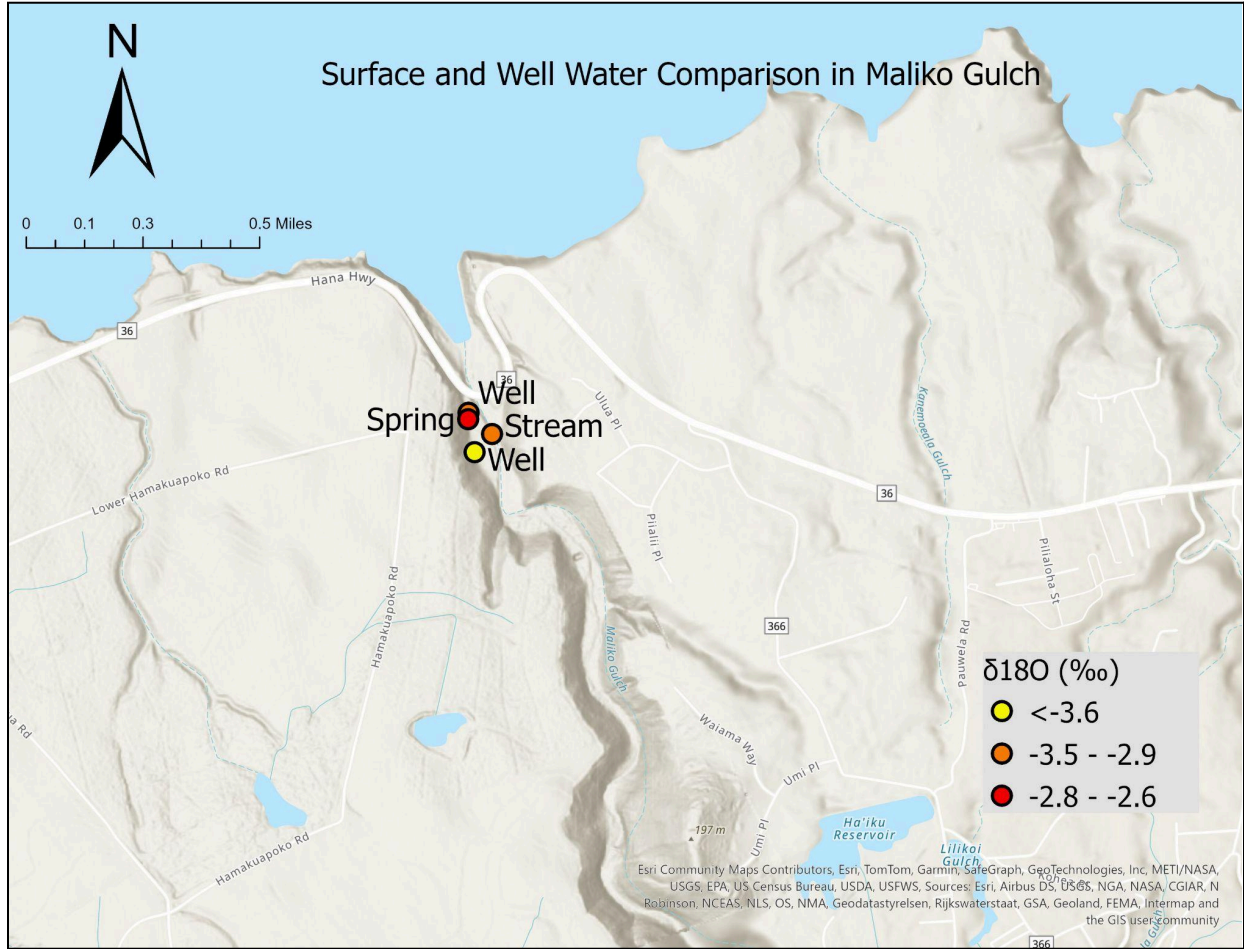


**Figure 24:** Water samples within Maliko Gulch.

Another intriguing area was Maliko Gulch located near the coast where there were multiple shallow wells, a stream, and spring in a close proximity, but varied isotopic content was found within. Two wells in close proximity to one another at a similar depth bore very different isotopic signatures, specifically  $\delta^{18}\text{O}$  content of  $-2.6\text{‰}$  and  $-3.5\text{‰}$  (see Figure 24). We theorized that the difference in isotopic content between these wells is likely caused by recharge from separate bodies and not saltwater intrusion because previous saltwater corrections indicated that saltwater intrusion had either none or a negligible effect on isotope values. The stream had the lowest salinity at  $15.84\text{ mg/L}$ . The spring was not able to be sampled for salinity due to limited available water for the YSI instrument. Although saltwater

corrections do not show saltwater intrusion playing a role in isotopic values, it is possible that saltwater intrusion does occur based on the groundwater being more saline than the surface water, especially near the coast. The small sample size of conductivity values may also limit the ability to see the full effect of saltwater intrusion. The well that shares similar isotope values with its nearby stream opposes Hypothesis 1, suggesting that wells may receive some recharge from springs. The other well supports Hypothesis 1 because of the difference in isotope values. We theorized that this implication demonstrates the existence of varied hydrogeology where some wells may receive an influx of recharge from streams while others may not.



**Figure 25:** Man made spring created by drilling into a cliff face 12 meters above the property.

The isotopic signature of the stream closely matches that of the well closest to the coast, likely indicating that the well may draw its water partly from the stream. The spring receives its water from a man made cave along the cliff face around 12 meters above the ground level that pumps water down to a spigot on the property, potentially signifying a different water source (see Figure 25). This is likely the reason that the spring has the most isotopically enriched signature compared to the other freshwater samples within the area. The heavily enriched signature supports the theory of varied hydrogeology within small areas that can

influence the isotopic values of wells. This spring is also known to receive irrigation water from the ditches and this will likely alter the isotope value significantly.

## Isotope Results in Reference to Previous Studies

Precipitation isotopes in Ha'ikū and Huelo were found to be enriched compared to both eastern Maui and Kilauea on Hawaii Island (Scholl et al., 1996; Scholl et al., 2002). The larger presence of enriched  $\delta^{18}\text{O}$  and  $\delta^2\text{H}$  isotopic content in our study area is likely due to its geographic position that leads to increased precipitation quantity. The areas sampled for precipitation by Scholl et al. contain locations on the leeward side of both Hawaii and Maui Island, meaning that the isotope content is more depleted, leading to a less enriched isotopic signature than northeast Maui (1996 & 2002).

Results found by Niu et al. (2017) suggested that basal and perched aquifers are separate and that wells do not vary temporally in northeast Maui stretching from Ha'ikū to Nahiku. This presented conflicting evidence found by Scholl et al. (2002) that found springs west of the Keanae Valley have a similar signature to deeper groundwater, suggesting a connected system. Although no confirmed perched aquifers were directly sampled in this study containing Ha'ikū and Huelo, it can be assumed that perched water bodies feed the surface water to an extent through springs and contribute to their isotopic signature. Differences in isotopic values were seen between surface water and groundwater in Ha'ikū, potentially also suggesting that these are two separate groups, agreeing with the findings of Niu et al. (2017). Huelo did not suggest a difference between the two groups, agreeing with the older theory proposed by Scholl et al. (2002).

In 2020, Niu et al. examined temporal variability in  $\delta^{18}\text{O}$  and  $\delta^2\text{H}$  in precipitation, springs, and the basal aquifer in the same study area as 2017 in northeastern Maui. Temporal variability was detected in precipitation and springs, but not the basal aquifer. Precipitation showed a strong temporal influence and wells did not exhibit a temporal influence in Ha'ikū and Huelo. Unfortunately, no springs were sampled continuously in this study for a comparison.

It is likely that seasonality in the composition of water isotopes in precipitation also play a role in causing shifts in the composition of groundwater throughout the year. Elevation is also known to influence the geochemical signature of a water source. Scholl et al. (1996 & 2002) found variation in stable freshwater isotopes at different elevations within northeast Maui and in Kilauea on Hawaii Island. Precipitation became more isotopically depleted in  $^{18}\text{O}$  content with increasing elevations in both locations. The findings within Ha'ikū and Huelo agree with Scholl et al. (1996 & 2002) as progressively higher elevation areas such as Haleakalā were more isotopically depleted than coastal areas such as Ha'ikū and Huelo.

## II. Hydrologic Framework and Groundwater Movement

Most groundwater in Ha'ikū has a geochemically distinct signature compared to its surface water. This suggests that there is little influence the streams have on the wells or the wells have on the streams. In contrast, the groundwater shows a very similar composition to the surface water within Huelo, signifying that the streams are possibly discharging baseflow from basal water. The similar composition may also signal that the aquifer is fully saturated, leading to similar values within each water source. The potential anomalies found within the study area highlight the highly varied hydrogeology within the study area that can cause differences in isotope composition within two of the same sources within a small area.

## III. Precipitation Changes with Reference to ENSO Phase Changes

El Niño appears to correlate with peaks in rainfall while La Niña appears to correlate with troughs in rainfall. One example is present near 2016 in Figure 22 during a strong El Niño that correlates with a sharp increase in precipitation during the rainy season. The effect of strong El Niño events on precipitation can also be seen in 1983, but is not seen during other recent strong El Niño events during 1997 or 2010. Strong La Niña events are not as pronounced with high peaks as El Niño events, but their impacts can be seen as they are typically present in troughs, or low points of precipitation in the rainfall record. For example,

the years 2000, 2008, and 2010 were briefly strong La Niña events that coincided with low quantities of precipitation. This signifies that ENSO phases do not seem to play a clear role in rainfall changes, but it is not the only factor because not every strong El Niño and increase in precipitation were concurrent. Other factors that may influence rainfall changes are anthropogenic climate change causing rising atmospheric temperatures and natural changes in atmospheric patterns. Less precipitation can lead to less recharge and more severe impacts from well withdrawals.

Several rain gauge station data showed significant deviations from the mean precipitation during El Niño years. This suggests that during El Niño years certain regions may experience pronounced changes in rainfall that may be attributed to shifts in atmospheric circulation patterns such as altered trade winds and changes in oceanic conditions. La Niña years showed a more mixed pattern of statistically significant results. This suggests that some regions experience significantly different rainfall during La Niña events, potentially due to local climate dynamics similarly to El Niño.

#### IV. Simulated Impacts on Existing Wells

Groundwater model simulations suggest that overall groundwater resources within Haiku and Huelo are likely to decrease to some extent as a result of future groundwater development. Most existing wells will likely not be heavily affected by an increase in groundwater withdrawals, depending on the placement and pumping rate of new wells. . Impacts of withdrawal on personal wells will depend greatly on proximity to locations of future wells and the quantity that it is pumping. The severity of impacts is very localized within Ha‘ikū as a result of the theorized locations of future wells based on selection criteria detailed within Maui County Ordinance 5335 (Maui County Department of Water Supply, 2019). According to the model, all wells are presented with some level of risk for problems withdrawing water due to decreases in nearly all scenarios.

# Conclusions

Based on the lack of a statistically significant relationship between groundwater and surface water quality parameters in the Haiku area, as shown in Table 3a, it appears unlikely that drawdown in basal water levels will impact stream baseflow, in Haiku specifically. In Huelo, the relationship between basal groundwater and stream baseflow is less clear. The majority of water samples from groundwater wells showed a more negative isotopic signature than the stream and spring samples, but there were outliers that could indicate surface water interactions with groundwater, especially within Huelo though it remains unclear if well withdrawals will or will not affect streams based on the potential connections between surface water and groundwater in Huelo.

Upon analysis of historical rainfall data, the areas of Ha'ikū and Huelo have experienced an overall decrease in precipitation since 1920, but most rainfall trends do not bear statistical significance. The only trend that had mostly consistent significance in every subregion excluding the Upper Slope was between 1980-2024 in the annual plots. The total rainfall has decreased annually between 1980-2024, except in the Upper Slope. The variability observed across the stations suggests that precipitation responds to climatic events like El Niño and La Niña are not uniform across regions. This supports the idea that regional climate factors such as topography, proximity to large bodies of water, and local wind patterns may play a significant role in determining how precipitation is affected by these global climatic events.

The results from model simulations of hypothetical groundwater development scenarios lowered the well head in each scenario. The magnitude of the impacts is highly dependent on the placement of pumping wells, the location of monitoring points and the rate of withdrawals.

# Acknowledgements

This project is for the communities of Ha‘ikū and Huelo, without whose support this project would have never been possible. The Ha‘ikū Community Association has shown great dedication to the care of their resources and has always been a helpful resource, able to offer plentiful information on the history of this area. We would like to thank donors from the Haiku Community that contributed personal funds to support the project, community members who provided access to wells and properties, the Haiku Community Association administration and board, along with the originators of the study, Lucienne DeNaie, Laf Young, Scott Werden, and Phil Lowenthal. This project has helped inspire others within the area to help the community further understand the health of their water resources.

## References

- Baalousha, Husam. (2012). Groundwater flow pattern in the Ruataniwha Plains as derived from the isotope and chemistry signature of the water. 10.13140/RG.2.1.2605.9366.
- Bassiouni, M., & Oki, D. S. (2013). Trends and Shifts in Streamflow in Hawai'i, 1913-2008. *Hydrological Processes*, vol. 27, no. 10, pp. 1484–500, <https://doi.org/10.1002/hyp.9298>.
- Boretti, A. & Rosa, L. (2019). Reassessing the projections of the World Water Development Report. *npj Clean Water* 2, 15. <https://doi.org/10.1038/s41545-019-0039-9>.
- Brewington, L., Keener, V., Mair, A. (2019). Simulating Land Cover Change Impacts on Groundwater Recharge under Selected Climate Projections, Maui, Hawai'i. *Remote Sensing*. 11(24):3048. <https://doi.org/10.3390/rs11243048>
- Chen, J., Theller, L., Gitau, M. W., Engel, B. A., & Harbor, J. M. (2017). Urbanization impacts on surface runoff of the contiguous United States. *Journal of Environmental Management*, 187, 470–481. <https://doi.org/10.1016/j.jenvman.2016.11.017>
- Davis, C. (2021). Return the water: In ongoing battle, Maui farmer finds water source locked up. Hawaii News Now.
- DeMaagd, N., & Roberts, M. J. (2021). How Will Climate Change Affect Residential Water Demand? Evidence from Hawai'i Microclimates. *Water Economics and Policy*, vol. 7, no. 1. <https://doi.org/10.1142/S2382624X21500053>.
- Frazier, A. G., & Giambelluca, T. W. (2017), Spatial trend analysis of Hawaiian rainfall from 1920 to 2012. *Int. J. Climatol.*, 37(5), 2522–2531. doi: 10.1002/joc.4862

Giambelluca, T. W., Chen, Q., Frazier, A. G., Price, J.P., Chen, Y. -L., Chu, P. -S., Eischeid, J. K., & Delparte, D. M. (2013). Online Rainfall Atlas of Hawai'i. Bull. Amer. Meteor. Soc. 94, 313-316, doi: 10.1175/BAMS-D-11-00228.1.

Gingerich, S. B. (2008). Maui County Department of Water Supply and Geological Survey, *Ground-water availability in the Wailuku area, Maui, Hawai'i*. U.S. Geological Survey.

Gingerich, S. B. (1999a). Groundwater and Surface Water in the Haiku Area, East Maui, Hawaii. USGS.

Gingerich, S. B. (1999b). Ground-Water Occurrence and Contribution to Streamflow, Northeast Maui, Hawaii. U.S. Department of the Interior, U.S. Geological Survey, 1999.

Gleick, P. H., & Palaniappan, M. (2010). Peak Water Limits to Freshwater Withdrawal and Use." Proceedings of the National Academy of Sciences - PNAS, vol. 107, no. 25, pp. 11155–62, <https://doi.org/10.1073/pnas.1004812107>.

Huang, Y. -F., Gayte, M., Tsang, Y., Longman, R. J., Nugent, A. D., Kodama, K., Lucas, M. P., & Giambelluca, T. W. (2022). Hourly rainfall data from rain gauge networks and weather radar up to 2020 across the Hawaiian Islands. figshare. Collection. <https://doi.org/10.6084/m9.figshare.c.5779532.v1>

Hui Alanui o Makena, The Sierra Club, & Mark Sheehan (2003). Consent Decree.

Hunt, C.D. and Rosa S.N. (2009). A multitracer approach to detecting wastewater plumes at Kihei and Lahaina, Maui, Hawaii. USGS Scientific Investigations Report 2009-5253, 166p. <http://pubs.usgs.gov/sir/2009/5253/>.

Izuka, S. K., Engott, J. A., Rotzoll, K., Bassiouni, M., Johnson, A. G., Miller, L. D., & Mair, A. (2018). Volcanic aquifers of Hawai‘i—Hydrogeology, water budgets, and conceptual models (ver. 2.0, March 2018): U.S. Geological Survey Scientific Investigations Report 2015-5164, 158 p., <https://doi.org/10.3133/sir20155164>.

Izuka, S.K., Rotzoll, K., and Nishikawa, T. (2021). Volcanic Aquifers of Hawai‘i—Construction and calibration of numerical models for assessing groundwater availability on Kaua‘i, O‘ahu, and Maui: U.S. Geological Survey Scientific Investigations Report 2020-5126, 63 p., <https://doi.org/10.3133/sir20205126>.

Johnson, A. G., Engott, J.A., Bassiouni, M., & Rotzoll, K. (2014). Spatially distributed groundwater recharge estimated using a water-budget model for the Island of Maui, Hawai‘i, 1978-2007.

Jones, B. D., Ladefoged, T. N., & Asner, G. (2015). Tracing the Resilience and Revitalisation of Historic Taro Production in Waipi‘o Valley, Hawai‘i. *The Journal of the Polynesian Society*, 124(1), 83–109. <http://www.jstor.org/stable/44733637>

Ke, X., Wang, W., Xu, X. et al., (2021). A saturated–unsaturated coupling model for groundwater flowing into seepage wells: a modeling study for groundwater development in river basins. *Environ Earth Sci* **80**, 711. <https://doi.org/10.1007/s12665-021-10035-8>

Keener, V. W., Marra, J. J., Finucane, M. L., Spooner, D., & Smith, M. H. (2012). Climate Change and Pacific Islands : Indicators and Impacts : Report for the 2012 Pacific Islands Regional Climate Assessment (PIRCA). Island Press, 2012.

Leščešen, I., Pantelić, M., Dolinaj, D., Stojanović, V., Milosevic, D. (2015). Statistical Analysis of Water Quality Parameters of the Drina River (West Serbia), 2004-11. *Polish Journal of Environmental Studies*. 24. 555-561. 10.15244/pjoes/29684.

Longman, R. J., Elison Timm, O., Giambelluca, T. W., & Kaiser, L. (2021). A 20-year analysis of disturbance-driven rainfall on O'ahu, Hawai'i. *Monthly Weather Review*.

<https://doi.org/10.1175/MWR-D-20-0287.1>

Longman, R.J., Ford, D.J., Anderson, A., Frazier, A.G, Giardina, C.P. (2023). Climate Change, Climate Variability, and Drought Portfolio. Pacific Drought Knowledge Exchange CCVD Series Version 5.2.

Longman, R. J., Lucas, M. P., Mclean, J., Cleveland, S., Kodama, K., Frazier, A. G., Kamelamela, K., Schriber, A., Dodge, M., Jacobs, G., Giambelluca, T. W. (n.d.). Hawai'i Climate Data Portal (HCDP). *Bulletin of the American Meteorological Society*.

Mair, A., Johnson A. G., Rotzoll, Kolja, and Oki, D. S. (2019). Estimated groundwater recharge from a water-budget model incorporating selected climate projections, Island of Maui, Hawai'i: U.S. Geological Survey Scientific Investigations Report 2019–5064, 46 p., <https://doi.org/10.3133/sir20195064>.

Maui County Department of Water Supply (2019). Maui, HI, Ordinance No. 5335.

Maui County Board of Water Supply (2021). Maui Island Plan Executive Summary for 2030 for Ordinance 5335.

<https://www.mauicounty.gov/DocumentCenter/View/84671/Executive-Summary?bidId=>

Maui County Department of Water Supply (n.d.). Unpublished Well Data.

Meyer, W. (2000). A Reevaluation of the Occurrence of Ground Water in the Nahiku Area, East Maui, Hawaii. U.S. Dept. of the Interior, U.S. Geological Survey.

Niu, Y., Castro, M. C., & Hall, C. M., Gingerich, S. B., Scholl, M. A. Warrier, R. B. (2017). Noble Gas Signatures in the Island of Maui, Hawaii: Characterizing Groundwater Sources in Fractured Systems: NOBLE GAS SIGNATURES IN MAUI, HAWAII. *Water Resources Research*, vol. 53, no. 5, pp. 3599–614, <https://doi.org/10.1002/2016WR020172>.

Niu, Y., Castro, M. C., Hall, C. M., Poulsen, C. J., Lohmann, K. C., & Aron, P. (2020). Groundwater sources in the Island of Maui, Hawaii — A combined noble gas, stable isotope, and tritium approach. *Applied Geochemistry*. 117. 104587. 10.1016/j.apgeochem.2020.104587.

Null, J. (2024). El Niño and La Niña Years and Intensities. <https://ggweather.com/enso/oni.htm>

Révész, K. & Coplen, T. B. (2008a). Determination of the delta ( $^2\text{H}/^1\text{H}$ ) of water: RSIL lab code 1574. In: Revesz, K., Coplen, T. B. (Eds.), *Methods of the Reston Stable Isotope Laboratory*. U.S. Geological Survey Techniques and Methods 10-C1, 27 p.

Révész, K. & Coplen, T. B. (2008b). Determination of the delta ( $^{18}\text{O}/^{16}\text{O}$ ) of water: RSIL lab code 489. In: Revesz, K., Coplen, T.B. (Eds.), *Methods of the Reston Stable Isotope Laboratory*. U.S. Geological Survey Techniques and Methods 10-C2, 28 p

Scholl, M. A., Ingebritsen, S. E., Janik, C. J., & Kauahikaua, J. P. (1996). Use of Precipitation and Groundwater Isotopes to Interpret Regional Hydrology on a Tropical Volcanic Island: Kilauea Volcano Area, Hawaii, *Water Resour. Res.*, 32(12), 3525-3537, Doi:10.1029/95WR02837., vol. 32, no. 12, 1996, pp. 3525–37, <https://doi.org/10.1029/95WR02837>.

Scholl, M. A., Gingerich, S. B., & Tribble, G. W. (2002). The Influence of Microclimates and Fog on Stable Isotope Signatures Used in Interpretation of Regional Hydrology: East

Maui, Hawaii. *Journal of Hydrology* (Amsterdam), vol. 264, no. 1, 2002, pp. 170–84, [https://doi.org/10.1016/S0022-1694\(02\)00073-2](https://doi.org/10.1016/S0022-1694(02)00073-2).

Scholl, M. A., Shanley, J. B., Murphy, S. F., Willenbring, J. K., Occhi, M., & Gonzáles, G. (2015). Stable-Isotope and Solute-Chemistry Approaches to Flow Characterization in a Forested Tropical Watershed, Luquillo Mountains, Puerto Rico. *Applied Geochemistry*, vol. 63, 2015, pp. 484–97, <https://doi.org/10.1016/j.apgeochem.2015.03.008>.

Shade, P. J. (1999). *Water Budget of East Maui, Hawaii* / Prepared in Cooperation with the County of Maui Department of Water Supply, State of Hawaii Commission on Water Resource Management. U.S. Dept. of the Interior, U.S. Geological Survey, 1999.

Stearns, H. T. & Macdonald, G. A. (1942). *Geology and Ground-Water Resources of the Island of Maui, Hawaii*. USGS.

Tachera, D. (2022). *A HYDROGEOCHEMICAL EXAMINATION OF WEST HAWAI‘I’S WATER CYCLE*. University of Hawai‘i at Manoa.

Timm, O. E., Giambelluca, T. W., & Diaz, H. F. (2015). Statistical Downscaling of Rainfall Changes in Hawai‘i Based on the CMIP5 Global Model Projections. *Journal of Geophysical Research*. Atmospheres, vol. 120, no. 1, 2015, pp. 92–112, <https://doi.org/10.1002/2014JD022059>.

Townsend, M. (2016). [Letter from Sierra Club member to United States of America Hawaii Senator].

Whittier, R. & El-Kadi, A. (2014). Human and Environmental Risk Ranking of Onsite Sewage Disposal Systems For the Hawaiian Islands of Kauai, Molokai, Maui, and Hawaii -

Final. Prepared by the University of Hawaii, Dept. of Geology and Geophysics for the State of Hawaii Dept. of Health, Safe Drinking Water Branch.

Xue, L., Wang, Y., Newman, A. J., Ikeda, K., Rasmussen, R. M., Giambelluca, T. W., Longman, R. J., Monaghan, A. J., Clark, M. P., & Arnold, J. R. (2020). How will rainfall change over Hawai'i in the future? High-resolution regional climate simulation of the Hawaiian Islands. *Bulletin Of Atmospheric Science And Technology*, 1, 459-490.  
doi:10.1007/s42865-020-00022-5.

Zhang, C., Wang, Y., Hamilton, K., & Lauer, A. (2016). Dynamical Downscaling of the Climate for the Hawaiian Islands. Part II: Projection for the Late Twenty-First Century. *Journal of Climate*, 29(23), 8333-8354. <https://doi.org/10.1175/JCLI-D-16-0038.1>

# Appendix

## I. Saltwater Correction Equation

$$C_1 = C_{mix} + (C_{mix} + C_2) \times (S_{mix} + S_1) / (S_2 - S_{mix})$$

$C_1$  represents the expected concentration or  $\delta$  value prior to seawater dilution.

$C_2$  represents the concentration or  $\delta$  value of the seawater endmember

$C_{mix}$  represents the concentration or  $\delta$  value that will be unmixed

$S_1$  represents the salinity of the fresh groundwater endmember

$S_2$  represents the salinity of the marine endmember

$S_{mix}$  represents the salinity of the sample to be unmixed

**Equation 1** adapted from Bishop (2015) after Hunt and Rosa (2009).

## II. Raw Isotope Data

### A. Sample Isotope Data from Wells, Springs, and Streams

#### 1. Streams

Sample Name	Sample Type	Date	$\delta^{18}\text{O}$ (‰)	$\delta^2\text{H}$ (‰)
Mehana Way	Stream	10/26/2022	-3.1	-8.9
Awalau S-1	Stream	2/27/2023	-4	-14.8
Honopou Stream	Stream	4/25/2023	-2.5	-5.2
Huelo Stream	Stream	3/29/2023	-2.8	-6.9
Kanemoeala-1	Stream	10/12/2022	-3	-9.5
Kealii-S-1	Stream	10/8/2022	-2.6	-5.9

M-S-1	Stream	2/27/2023	-3.1	-9.7
Maliko 5/6 Waterfall	Stream	7/30/2023	-2.6	-6.8
Ohia S-1	Stream	2/27/2023	-3.1	-9.2
Twin Falls	Stream	11/2/2023	-2.6	-5.4
Twin Falls	Stream	12/1/2023	-5.8	-30.9
Twin Falls D	Stream	12/1/2023	-5.8	-31
Twin Falls S-1	Stream	3/29/2023	-2.9	-7
Twin Falls S-2	Stream	4/25/2023	-2.7	-6.6
Twin Falls Stream 3	Stream	5/30/2023	-2.7	-4.9
Twin Falls D	Stream	5/30/2023	-2.7	-4.8
Twin Falls	Stream	1/3/2024	-2.9	-6.4
Twin Falls D	Stream	1/3/2024	-2.9	-6.4
Twin Falls	Stream	2/8/2024	-2.8	-5.1
Twin Falls	Stream	4/1/2024	-2.7	-5.3
Twin Falls	Stream	5/30/2023	-2.7	-4.8
Twin Falls	Stream	2/29/2024	-3	-3.4
Huelo	Stream	4/30/2024	-2.8	-5.7
Huelo	Stream	6/4/2024	-2.4	-3.4
Huelo	Stream	7/1/2024	-2.7	-5.6
West K Ditch	Stream	7/30/2023	-2.7	-5.9
West K S	Stream	9/27/2023	-2.5	-5.5
West K S	Stream	11/2/2023	-2.5	-6
West K S	Stream	12/1/2023	-2.8	-5.4
West K S	Stream	2/29/2024	-2.5	-3.7
West K S	Stream	4/1/2024	-2.6	-5
West K S-1	Stream	2/27/2023	-3.2	-10.8
West K S-2	Stream	2/27/2023	-2.9	-7.5
West K S-3	Stream	3/29/2023	-2.9	-7.5

## 2. Springs

Sample Name	Sample Type	Date	$\delta^{18}\text{O}$ (‰)	$\delta^2\text{H}$ (‰)
Hokoana Spring 1	Spring	10/5/2022	-2.6	-5.4
Honopou Spring	Spring	4/25/2023	-2.7	-5.7
Maliko Sp	Spring	7/30/2023	-2.7	-7.5
Papalua Sp-1	Spring	10/4/2022	-2.5	-4.9
Phi's Spring-2	Spring	10/8/2022	-2.7	-6
Phil Pond	Spring	6/27/2023	-2.6	-5.5
Phil Spring	Spring	6/27/2023	-2.7	-6.1
Phil Spring April	Spring	4/1/2024	-2.8	-6.5
Phil's Spring-1	Spring	10/8/2022	-2.7	-5.6
Waha Sp-1	Spring	10/4/2022	-2.9	-8.6
West K Sp	Spring	7/30/2023	-2.6	-6.3
West K Sp 2	Spring	7/30/2023	-2.8	-6.6
West K Sp 3	Spring	7/30/2023	-2.7	-5.9

## 3. Wells

Sample Name	Sample Type	Date	$\delta^{18}\text{O}$ (‰)	$\delta^2\text{H}$ (‰)
Awalau W-1	Well	2/27/2023	-3.2	-10
BF 2-19-A February	Well		-2.7	-2
Five Corners	Well	3/29/2023	-3.3	-10.3
Five Corners	Well	12/1/2023	-3.5	-12.3
Five Corners	Well	1/3/2024	-3.4	-11.4
Five Corners	Well	2/8/2024	-3.4	-11.1
Five Corners	Well	2/29/2024	-3.4	-10.5
Five Corners D	Well	1/3/2024	-3.4	-10.7

Five Corners W-1	Well	10/9/2022	-3.3	-10.3
Five Corners W-2	Well	6/27/2023	-3.3	-10.5
Frank Felton Well 1	Well	10/5/2022	-3.4	-10.9
HTA-1	Well	10/8/2022	-3.6	-13.5
Hokoana Well 1	Well	10/5/2022	-2.9	-8.9
Hono 2-19-A 99 February	Well		-2.6	-2.8
Huelo W June	Well	6/27/2023	-2.6	-6.5
Huelo W June D	Well	6/27/2023	-2.7	-6.7
Huelo W July	Well	8/1/2023	-2.6	-6.9
Huelo W September	Well	9/27/2023	-2.7	-6.8
Huelo W-1	Well	10/9/2022	-2.7	-7.6
Huelo W October	Well	11/2/2023	-2.7	-7.1
Huelo W November	Well	12/1/2023	-2.7	-7.3
Huelo W December	Well	1/3/2024	-2.7	-6.7
Huelo W February	Well	2/8/2024	-2.7	-6.9
Huelo W February	Well	2/29/2024	-2.7	-7.5
Huelo W	Well	4/1/2024	-2.5	-5.9
Huelo	Well	4/30/2024	-2.5	-6.5
Huelo	Well	6/4/2024	-2.6	-6.4
Huelo	Well	6/4/2024	-2.6	-6.5

Huelo	Well	7/1/2024	-2.6	-6.4
Huelo	Well	7/1/24	-2.5	-6.3
Maliko-w-1	Well	10/9/2022	-3.6	-13.5
Martin Well 1	Well	10/5/2022	-3.3	-10.3

#### 4. Precipitation

Sample Name	Sample Type	Date	$\delta^{18}\text{O}$ (‰)	$\delta^2\text{H}$ (‰)
Haleakala P-3	Precipitation	5/30/2023	-3.8	-16.3
Haleakala P-3 D	Precipitation	5/30/2023	-3.9	-16.7
Haleakala P-4	Precipitation	5/30/2023	-4.1	-18.7
Haleakala P-5	Precipitation	7/30/2023	-5.6	-35.2
Haleakala P-6	Precipitation	8/30/2023	-2.5	-15.4
Haleakala P-7	Precipitation	9/27/2023	-3.1	-11.2
Haleakala P-9	Precipitation	12/1/2023	-8.5	-55
Haleakala P-10	Precipitation	1/3/2024	-5	-19.9
Haleakala P-11	Precipitation	2/8/2024	-5.5	-30.5
Haleakala P-12	Precipitation	2/29/2024	-4	-16.8
Haleakala P-13	Precipitation	4/1/2024	-5.3	-27.4
Haleakala	Precipitation	4/30/2024	-3.8	-16.9
Haleakala	Precipitation	6/4/2024	-4.2	-21.5
Haleakala	Precipitation	7/1/2024	-5.6	-34.8
Huelo P-1	Precipitation	3/29/2023	-2.9	-10.3
Huelo P-2	Precipitation	4/24/2023	-2.7	-8.2
Huelo P-3	Precipitation	5/30/2023	-2.5	-3.5
Huelo P-4	Precipitation	5/30/2023	-1.2	2.6
Huelo P-5	Precipitation	7/30/2023	-1.6	-1.4
Huelo P-6	Precipitation	8/30/2023	-1.9	-2.4
Huelo P-7	Precipitation	9/27/2023	-1.9	-2.3
Huelo P-8	Precipitation	11/2/2023	-1.8	-1.1

Huelo P-9	Precipitation	12/1/2023	-6.5	-38.7
Huelo P-10	Precipitation	1/3/2024	-1.8	3
Huelo P-11	Precipitation	2/8/2024	-2.2	-0.7
Huelo P-12	Precipitation	2/29/2024	-1.3	8.8
Huelo P-12 D	Precipitation	2/29/2024	-1.3	9.4
Hulelo P-13	Precipitation	4/1/2024	-1.8	3
Huelo	Precipitation	4/30/2024	-1.7	-1
Huelo	Precipitation	6/4/2024	-1.7	-0.7
Huelo	Precipitation	7/1/2024	-1.9	-4.1
Paia P-1	Precipitation	4/25/2023	-1.4	-3.9
Paia P-2	Precipitation	5/30/2023	-1.2	3.3
Paia P-3	Precipitation	6/27/2023	-1.2	3.5
Paia P-4	Precipitation	7/30/2023	-1.4	-3.9
Paia P-5	Precipitation	8/30/2023	-0.9	4.1
Paia P-6	Precipitation	9/27/2023	-1.2	1.9
Paia P-7	Precipitation	11/2/2023	-4.4	-26
Paia P-8	Precipitation	12/1/2023	-2.2	-3.1
Paia P-9	Precipitation	1/3/2024	-1.6	3.7
Paia P-10	Precipitation	2/8/2024	-3	-12.3
Paia P-11	Precipitation	2/29/2024	-0.5	13.9
Paia P-11 D	Precipitation	2/29/2024	-0.9	4.1
Paia P-12	Precipitation	4/1/2024	-0.9	8
Piiholo P-1	Precipitation	3/29/2023	-2.9	-6.2
Piiholo P-2	Precipitation	4/24/2023	-3.3	-15.5
Piiholo P-3	Precipitation	5/30/2023	-2.6	-4
Piiholo P-4	Precipitation	6/30/2023	-2.1	-1.7
Piiholo P-5	Precipitation	7/30/2023	-2.6	-6.9
Piiholo P-6	Precipitation	8/30/2023	-1.2	1.8
Piiholo P-7	Precipitation	9/27/2023	-1.8	-1.2

Piiholo P-8	Precipitation	11/2/2023	-2.9	-17.5
Piiholo P-9	Precipitation	12/1/2023	-2.9	-5.8
Piiholo P-9 D	Precipitation	12/1/2023	-2.9	-5.6
Piiholo P-10	Precipitation	1/3/2024	-2.4	1.6
Piiholo P-11	Precipitation	2/8/2024	-3.4	-10.5
Piiholo P-11 D	Precipitation	2/8/2024	-3.3	-10.1
Piiholo P-12	Precipitation	2/29/2024	-1.7	6.2
Piiholo P-13	Precipitation	4/1/2024	-2.7	-4.6
Piiholo P-14	Precipitation	6/4/2024	-2.9	-10.7
Piiholo P-14 D	Precipitation	6/4/2024	-2.8	-10.5
Piiholo P-15	Precipitation	7/1/2024	-3.3	-15.8
Haiku P-1	Precipitation	3/29/2023	-2.5	-5.5
Haiku P-2	Precipitation	4/24/2023	-3.4	-17.4
Haiku P-3	Precipitation	5/30/2023	-2.2	-1.6
Haiku P-4	Precipitation	6/27/2023	-1.8	0.8
Haiku P-5	Precipitation	7/30/2023	-2.6	-6.6
Haiku P-6	Precipitation	8/30/2023	-1.6	0.1
Haiku P-7	Precipitation	9/27/2023	-1.9	-2
Haiku P-9	Precipitation	12/1/2023	-2.9	-9
Haiku P-10	Precipitation	1/3/2024	-1.9	2.4
Haiku P-11	Precipitation	2/8/2024	-2.5	-3.1
Haiku P-12	Precipitation	2/29/2024	-1.5	8.5
Haiku P-12 D	Precipitation	2/29/2024	-1.5	8.6
Haiku	Precipitation	4/1/24	-1.7	4.5
Haiku	Precipitation	4/30/2024	-1.9	-0.9
Haiku	Precipitation	6/4/2024	-1.7	-0.7
Haiku	Precipitation	7/1/2024	-2.2	-6.6

B. Isotope Statistics for all Samples

Isotope	Min	Max	Mean	Median
$\delta^{18}\text{O}$ (‰)	-8.50	-0.50	-2.77	-2.70
$\delta^2\text{H}$ (‰)	-55.00	13.90	-7.36	-6.40

III. Major Ion Concentrations in Springs, Streams, and Wells

A. Stream and Spring Major Ion Concentrations

Type	Stream	Stream	Spring	Spring	Spring	Spring	Spring
Longitude	-156.290	-156.307	-156.339	-156.327	-156.275	-156.275	-156.267
Latitude	20.882	20.904	20.933	20.942	20.912	20.913	20.911
Fluoride (mg/L)	0.026	0.033	0.729	0.587	0.037	0.044	0.07
Chloride (mg/L)	7.25	13.4	35.49	30.86	17.29	19.07	17.03
Nitrite (mg/L)	0	0	0	0.037	0	0	0
Bromide (mg/L)	0.03	0.08	0.19	0.47	0.11	0.1	0.07
Nitrate (mg/L)	0.24	1.07	10.13	42.23	3.17	3.53	0.74
Phosphate (mg/L)	0	0	2.79	1.76	0.08	0.1	0.09
Sulfate (mg/L)	1.61	4.16	25.38	20.27	5.63	6.26	4.11
Lithium (mg/L)	0	0	0	0	0	0	0
Sodium (mg/L)	5.12	9.82	62.6	65.83	12.04	13.24	14.32
Ammonium (mg/L)	0.005	0.002	0.008	0.034	0.002	0.002	0.005
Potassium (mg/L)	0.68	1.3	2.3	3.31	0.97	1.08	1.18
Magnesium (mg/L)	1.25	2.57	3.09	1.93	2.81	3.12	4.05
Calcium (mg/L)	1.58	2.78	3.36	2.3	3.29	3.59	4.77

Type	Stream	Spring	Stream	Spring	Stream	Stream	Spring
Longitude	-156.266	-156.280	-156.338	-156.250	-156.252	-156.312	
Latitude	20.923	20.917	20.933	20.903	20.908	20.916	
Fluoride (mg/L)	0.031	0.035	0.039	0.017	0.02	0.031	0.004
Chloride (mg/L)	23.58	8.37	15.84	12.85	11.46	12.46	2.21
Nitrite (mg/L)	0	0	0.004	0	0	0	0
Bromide (mg/L)	0.14	0.05	0.1	0.1	0.08	0.07	0
Nitrate (mg/L)	0.27	0.51	1.68	0.61	0.02	1.51	0.16
Phosphate (mg/L)	0	0.03	0.04	0	0	0.05	0
Sulfate (mg/L)	5.81	2.32	4.95	4.94	2.59	3.78	0.34
Lithium (mg/L)	0	0	0	0	0	0	0
Sodium (mg/L)	15.76	6.27	12.05	8.08	7.9	8.53	0.35
Ammonium (mg/L)	0.007	0.004	0.002	0.001	0.001	0.003	0.001
Potassium (mg/L)	0.97	0.66	1.58	0.38	0.53	1.12	0.03
Magnesium (mg/L)	3.64	1.91	2.91	1.41	1.83	2.14	0.15
Calcium (mg/L)	2.36	2.43	3.04	1.44	1.85	2.29	0.25

#### B. Well Major Ion Concentrations

Type	Well	Well	Well	Well	Well	Well
Longitude	-156.286	-156.277	-156.325	-156.306	-156.339	-156.220
Latitude	20.879	20.935	20.918	20.913	20.933	20.914
Fluoride (mg/L)	0.024	0.148	0.144	0.059	0.309	0.087

Chloride (mg/L)	8.36	150.46	137.21	43.65	138.49	49.44
Nitrite (mg/L)	0	0	0	0	0	0
Bromide (mg/L)	0.04	0.54	0.59	0.01	0.63	0.23
Nitrate (mg/L)	0.49	2.33	11.28	3.15	9.53	3.47
Phosphate (mg/L)	0	0	0.21	0.14	0.44	0.22
Sulfate (mg/L)	2.29	21.39	21.01	6.76	40.19	10.35
Lithium (mg/L)	0	0	0	0	0	0
Sodium (mg/L)	6.26	81.73	78.69	26.37	109.7	30.1
Ammonium (mg/L)	0.001	0.007	0.007	0.001	0.396	0.001
Potassium (mg/L)	0.65	4.31	5.17	2.54	5.46	1.43
Magnesium (mg/L)	1.93	14.64	13.84	7.88	19.52	5.55
Calcium (mg/L)	2.47	11.33	15.95	10.62	25.59	5.36

Type	Well						
Longitude	-156.335	-156.274	-156.287	-156.335	-156.277	-156.339	-156.278
Latitude	20.935	20.932	20.913	20.935	20.936	20.932	20.933
Fluoride (mg/L)	0.091	0.065	0.061	0.091	0.066	0.129	0.036
Chloride (mg/L)	201.37	106.29	29.8	204.53	269.95	280.72	46.58
Nitrite (mg/L)	0	0	0	0	0	0	0.009
Bromide (mg/L)	0.73	0.44	0.13	0.74	0.98	1.06	0.18
Nitrate (mg/L)	5.57	7.47	3.07	5.87	2.66	7.84	1.14

Phosphate (mg/L)	0.19	0.19	0.16	0.26	0.11	0.26	0.05
Sulfate (mg/L)	29.97	16.89	5.09	30.43	38.45	43.26	5.67
Lithium (mg/L)	0	0	0	0	0	0	0.001
Sodium (mg/L)	118.76	74.69	19.93	120.83	149.76	161.58	27.88
Ammonium (mg/L)	0.001	0.001	0.002	0.001	0.004	0.005	0.074
Potassium (mg/L)	6.61	3.31	2.07	6.73	6.98	8.42	1.79
Magnesium (mg/L)	16.88	10.07	7.4	17.15	23.2	23.74	6.57
Calcium (mg/L)	16.44	10.73	10.87	16.59	16.71	18	6.12

### C. Ion Statistics

Ion	Min	Max	Mean	Median
Fluoride (mg/L)	0.00	0.73	0.11	0.06
Chloride (mg/L)	2.21	280.72	68.64	28.83
Nitrite (mg/L)	0.00	0.06	0.00	0.00
Bromide (mg/L)	0.00	1.06	0.29	0.14
Nitrate (mg/L)	0.02	42.23	4.67	2.50
Phosphate (mg/L)	0.00	2.79	0.26	0.10
Sulfate (mg/L)	0.34	43.26	13.27	6.04
Lithium (mg/L)	0.00	0.00	0.00	0.00
Sodium (mg/L)	0.35	161.58	45.86	23.15
Ammonium (mg/L)	0.00	0.48	0.04	0.00
Potassium (mg/L)	0.00	8.42	2.56	1.51
Magnesium (mg/L)	0.15	23.74	7.44	3.85
Calcium (mg/L)	0.25	25.59	7.64	4.18

D. Locations of Water Sources Compared between Haiku and Huelo

Location	Sample Type	Sample Number
Huelo	Well	1
Huelo	Stream	2
Ha'ikū	Well	3
Ha'ikū	Stream	4

IV. Paired t-test testing for significance of the relationship between individual ENSO events compared to all ENSO events.

Station	Year	El Niño Precipitation	El Niño Significance	El Niño p-value	La Niña Precipitation	La Niña Significance	La Niña p-value
Haiku	1994	232.918	D	0.000316			
Haiku	1995				502.92	D	0.002248
Haiku	1996				637.286	D	0.034847
Haiku	1997	651.764	D	0.032381			
Haiku	1998				934.72	N	0.5062
Haiku	1999				1368.298	D	0.000142
Haiku	2000				1237.234	D	0.001997
Haiku	2001				1223.264	D	0.002666
Haiku	2002	1057.148	N	0.764197			
Haiku	2003	1077.976	N	0.661135			
Haiku	2004	1525.778	D	0.005402			
Haiku	2005				1435.862	D	3.93E-05
Haiku	2006	1175.512	N	0.287575			
Haiku	2007				1086.104	D	0.043185
Haiku	2008				869.95	N	0.978384

Haiku	2009	1050.29	N	0.799345			
Haiku	2010				972.82	N	0.303497
Haiku	2011				757.936	N	0.287548
Haiku	2012				903.732	N	0.717714
Haiku	2013				965.454	N	0.337315
Haiku	2014	1281.938	N	0.093121			
Haiku	2015	413.004	D	0.002055			
Haiku	2016				0	D	2.81E-07
Haiku	2017				814.324	N	0.601358
Haiku	2018	1902.714	D	0.000111			
Haiku	2019	767.08	N	0.12212			
Haiku	2020				165.608	D	3.75E-06
Pukalani	1994	74.676	D	0.00318			
Pukalani	1995				250.19	D	0.049851
Pukalani	1996				612.648	D	2.62E-05
Pukalani	1997	550.164	N	0.727189			
Pukalani	1998				235.966	D	0.027012
Pukalani	1999				219.71	D	0.013099
Pukalani	2000				485.14	D	0.007142
Pukalani	2001				410.21	N	0.170649
Pukalani	2002	777.494	D	0.039011			
Pukalani	2003	344.678	N	0.174253			
Pukalani	2004	976.884	D	0.002007			
Pukalani	2005				699.77	D	1.00E-06
Pukalani	2006	389.636	N	0.312268			
Pukalani	2007				508	D	0.002509
Pukalani	2008				297.434	N	0.297898
Pukalani	2009	240.284	D	0.038081			
Pukalani	2010				355.6	N	0.828782

Pukalani	2011				289.56	N	0.228976
Pukalani	2012				62.484	D	1.37E-05
Pukalani	2013				172.466	D	0.001517
Pukalani	2014	0	D	0.001112			
Pukalani	2015	994.41	D	0.001569			
Pukalani	2016				406.146	N	0.19753
Pukalani	2017				443.484	D	0.045433
Pukalani	2018	1004.316	D	0.001367			
Pukalani	2019	254	D	0.046846			
Pukalani	2020				83.058	D	3.11E-05
Waikamoi	1994	1391.92	D	0.009098			
Waikamoi	1995				3515.36	N	0.09626
Waikamoi	1996				4142.74	D	0.002068
Waikamoi	1997	3827.78	N	0.090086			
Waikamoi	1998				3530.6	N	0.088492
Waikamoi	1999				2776.22	N	0.61522
Waikamoi	2000				3139.44	N	0.550357
Waikamoi	2001				4513.58	D	0.000206
Waikamoi	2002	3454.4	N	0.299496			
Waikamoi	2003	4536.44	D	0.007239			
Waikamoi	2004	5044.44	D	0.001286			
Waikamoi	2005				4907.28	D	2.09E-05
Waikamoi	2006	4259.58	D	0.019435			
Waikamoi	2007				2806.7	N	0.681188
Waikamoi	2008				1572.26	D	0.000713
Waikamoi	2009	2695.448	N	0.63121			
Waikamoi	2010				1877.568	D	0.00491
Waikamoi	2011				2371.852	N	0.097918
Waikamoi	2012				4369.054	D	0.0005

Waikamoi	2013				3505.962	N	0.101344
Waikamoi	2014	4051.3	D	0.041039			
Waikamoi	2015	581.406	D	0.000603			
Waikamoi	2016				2808.478	N	0.685128
Waikamoi	2017				564.642	D	2.37E-06
Waikamoi	2018	1325.118	D	0.007183			
Waikamoi	2019	1082.802	D	0.003097			
Waikamoi	2020				671.068	D	4.08E-06
Kaupakulua	1994	861.06	D	5.34E-05			
Kaupakulua	1995				2428.24	N	0.360381
Kaupakulua	1996				2725.42	N	0.229574
Kaupakulua	1997	3738.88	D	0.003623			
Kaupakulua	1998				3116.58	D	0.000868
Kaupakulua	1999				2918.46	D	0.017169
Kaupakulua	2000				2745.74	N	0.181087
Kaupakulua	2001				2608.58	N	0.702668
Kaupakulua	2002	2423.16	N	0.333906			
Kaupakulua	2003	2400.3	N	0.297715			
Kaupakulua	2004	2415.54	N	0.321492			
Kaupakulua	2005				2192.02	D	0.016826
Kaupakulua	2006	1943.1	D	0.020005			
Kaupakulua	2007				2268.22	N	0.050524
Kaupakulua	2008				1958.34	D	0.000501
Kaupakulua	2009	2400.808	N	0.298486			
Kaupakulua	2010				1781.048	D	4.01E-05
Kaupakulua	2011				2510.79	N	0.743373
Kaupakulua	2012				2659.888	N	0.454273
Kaupakulua	2013				2547.874	N	0.95336
Kaupakulua	2014	3556.762	D	0.011001			

Kaupakulua	2015	3793.49	D	0.002621			
Kaupakulua	2016				3932.174	D	4.00E-08
Kaupakulua	2017				2798.318	N	0.093467
Kaupakulua	2018	3678.174	D	0.005221			
Kaupakulua	2019	2510.028	N	0.500537			
Kaupakulua	2020				1703.07	D	1.42E-05
Total # D			27D		34D		
Total # N			17N		29N		

The results include the p-values for both total and mean precipitation, along with labels indicating whether the event precipitation data for each year was significantly different ("D") from the whole or not ("N") from the average precipitation during the respective climatic event. The La Niña and El Niño Result columns show whether each year's precipitation significantly deviated from the average precipitation for these events. There is a larger total number of 'D' values than 'N,' meaning that most individual ENSO phases are unlikely to share a relationship with the majority of the ENSO phases.